Plio-Quaternary tectonic evolution of the southern margin of the Alboran Basin (Western Mediterranean)

Manfred Lafosse[1,*], Elia d'Acremont[1], Alain Rabaute[1], Ferran Estrada[2], Martin Jollivet-Castelot[3], Juan Tomas Vazquez [4], Jesus Galindo-Zaldivar [5,6], Gemma Ercilla[2], Belen Alonso[2], Abdellah Ammar[7], Christian Gorini [1]

[1] Sorbonne Université, CNRS-INSU, Institut des Sciences de la Terre Paris, ISTeP UMR 7193, F-75005 Paris, France
[2] Instituto de Ciencias del Mar, ICM-CSIC, Continental Margin Group, 08003 Barcelona, Spain
[3] Univ. Lille, CNRS, Univ. Littoral Côte d'Opale, UMR 8187, Labratoire d'Océanologie et de Géosciences (LOG), F59000, Lille, France
[4] Instituto Espanol de Oceanografıa, C.O.Malaga, Fuengirola, Spain
[5] Dpto. de Geodinamica, Universidad de Granada, Granada, Spain.
[6] Instituto Andaluz de Ciencias de la Tierra (CSIC-UGR), Granada, Spain.
[7] Université Mohammed V-Agdal, Rabat, Morocco
[*]now at: Tectonic and Structural Geology Groups, Department of Earth Sciences, Utrecht University, PO Box 80.021, 3508 TA Utrecht, The Netherlands

Correspondence to: Manfred Lafosse (m.r.lafosse@uu.nl)

Abstract. Progresses in the understanding of the sedimentary dynamic of the Western Alboran Basin lead us to propose a model of the evolution of its tectonic evolution since the Pliocene to the present time. Extensional and strike-slip structures accommodate the Miocene back-arc extension of the Alboran Basin but undergo progressive tectonic inversion since the Tortonian. Across the Alboran Basin, the Alboran Ridge becomes a transpressive structure accommodating the shortening. We map its southwestern termination: a Pliocene rhombic structure exhibiting series of folds and thrusts. It is crossed by a younger strike-slip structure, the Al-Idrissi fault zone (AIF). The AIF is a Pleistocene to the present-day active fault zone, which crosses the Alboran Ridge and connects southward to the transtensive Nekor Basin and the Nekor fault. In the Moroccan shelf and at the edge of a submerged volcano, we date the inception of the local shelf subsidence from the 1.81-1.12 Ma. It marks the propagation of the AIF toward the Nekor Basin. Pliocene thrusts and folds and Quaternary transtension appear at first sight as different tectonic periods but reflects the long-term evolution of a transpressive system. Despite a constant direction of Africa/Eurasia convergence since 5Ma at the scale of the southern margin of Alboran Basin, the Pliocene-Quaternary compression evolves from transpressive to transtensive on the AIF and the Nekor Basin. This system reflects the expected evolution of the deformation of the Alboran Basin under the indentation of the African lithosphere.

1. Introduction

In a brittle regime, oblique compression leads to strain partitioning between lateral motion and efficient rock uplifts (Fossen et al., 1994; Fossen and Tikoff, 1998). With time, the simple shear deformation involves blocks rotation and changes in the local stress field, leading to the formation of better oriented tectonic structures (Nur et al., 1986; Ron et al., 2001; Scholz et al., 2010). It often results in an intricate pattern of distributed deformation with transpressive and transtensive structures. The Alboran Basin is a typical example of such a complex tectonic evolution.

The Alboran Basin develops over a collapsed Tertiary orogen and corresponds to internal units of the Betic-Rif belt (Fig. 1) (Comas et al., 1999), and together form what we call the Alboran tectonic domain. The formation of the Alboran Basin has been linked to back-arc extension and lithospheric tearing during early Miocene (e.g., Jolivet et al., 2009, 2008). Since the Miocene, several strike-slip shear zones running from the Iberian to the Moroccan margins accommodate the upper-plate deformation forming a broad shear zone called the Trans-Alboran Shear Zone (TASZ; Fig. 1)(Leblanc and Olivier, 1984).

Following the westward slab retreat during Miocene time, the TASZ behaves as a left-lateral transfer fault zone accommodating the extension of the Alboran Basin. The Africa-Eurasia NW-SE oblique convergence leads to a tectonic

45   reorganization during the Late Miocene (Comas et al., 1999; Do Couto et al., 2016). Due to ongoing Africa-Eurasia convergence, the TASZ underwent an oblique positive inversion starting around 8 Ma in the Betic Margin of the Bas Basin (Do Couto et al., 2014; Martínez-García et al., 2017). The compression migrates westward in relation to the slab roll-back, since approximately 7-8 Ma from the Algerian margin to the Alboran Ridge, and since ca. 5 Ma on the Al-Idrissi fault (Fig. 1 and 2) (Giaconia et al., 2015).

50   Several authors shows the moderate oblique convergence relatively to the principal tectonic structures of the TASZ. DeMets et al. (2015) showed that it is possible to constraint very precisely the location of the rotation poles between Eurasia, North America, and Africa since the Miocene. The migration of the rotation pole between Africa and Eurasia toward the SE during the Pliocene and the Quaternary results in a roughly constant direction of Africa-Eurasia convergence, an increase in the convergence rates from approximately ~3.5 mm/y to ~5.5 mm/y at 35° N / 5° W between 5.2 Ma and present-day, respectively

55   (DeMets et al., 2015). More recently, Spakman et al., (2018) show that from 8 Ma to present-day, the Africa – Eurasia absolute convergence produces 15km of relative motion between Africa and Eurasia in the NNE-SSW direction.

However, changes in stress direction are demonstrated in the Betic-Rif belt during the Plio-Quaternary (Aït Brahim and Chotin, 1990; Galindo-Zaldívar et al., 1993; Giaconia et al., 2015; Martínez-Díaz and Hernández-Enrile, 2004). In the Rif, field studies and paleomagnetic data demonstrate a 20° counter clock-wise rotation since the upper-Miocene (Crespo-Blanc et al., 2016;

60   Platt et al., 2003). The change in horizontal stress directions has led to compression and uplift of Plio-Quaternary sediments offshore the Palomares fault on the Iberian Margin (Giaconia et al., 2015). At present-time, the direction of shortening seems orthogonal to the NE-SW structures of the TASZ (Fig. 1)(Palano et al., 2013). Using a block rotation pinned model, Meghraoui and Pondrelli, (2013) propose that oblique convergence leads to a rigid block rotation accommodated by transcurrent faults (e.g. the TASZ, Fig. 1).

65   Besides, the distribution of the seismicity in the western part of the Betic-Rif belt reveals complex geodynamic interactions. Deep earthquakes occur at depths >60 km (Fig. 2a). They are located in the central Betic, beneath the West Alboran Basin (WAB), and the Rif Mountains (Fig. 1), and are associated to a sinking slab (Fig. 2a) (Bezada et al., 2013; Ruiz-Constán et al., 2011; Thurner et al., 2014). In addition to the Africa-Eurasia convergence, lithospheric scale processes and crustal heterogeneities such as mantel and lower crust delamination can have a strong influence on the deformation and the structure

70   of the Alboran Basin (Petit et al., 2015; Thurner et al., 2014). The mechanical coupling between the Alboran Domain and the subsiding lithosphere (e.g. Perouse et al., 2010; Neres et al., 2016) , and/or slab dragging under Africa/Eurasia convergence (Spakman et al., 2018) could cause the extrusion the Betico-Rifian belt toward the South-West (e.g. Petit et al., 2015; Thurner et al., 2014).

The Africa-Eurasia plate boundary in the Alboran Basin and the Betic - Rif belt cannot be assigned to a single fault system

75   (Fadil et al., 2006), and some authors proposed to define a present-day diffuse plate boundary between Africa and Eurasia (e.g., Palano et al., 2015). At the crustal level, recent progress in structural mapping have shown that the distribution of the deformation in the Alboran Sea switched from the Tortonian NE-SW to Quaternary NNE-SSW faults (Estrada et al., 2018; Galindo-Zaldivar et al., 2018; Lafosse et al., 2017; Martínez-García et al., 2013, 2017). On the Averroes Fault (Fig. 1), the estimate of the age of strike-slip deformation is around 1Ma (Perea et al., 2018). However, the timing and the mechanism of

80   this structural evolution remains poorly constraints.

In the present work, we address the structural evolution of the southwestern margin of the Alboran Basin toward the termination of the TASZ through the Plio-Quaternary. We analysis multi-resolution 2D seismic reflection data, TOPAS profiles, and multibeam data. Based on our recent dataset and our seismic stratigraphic interpretation, we observe that the structural subdivision of the Alboran Basin and its margin may reflect a Pleistocene change in tectonic style. We propose a new tectonic

85   model explaining the evolution of the SAR and the Al-Idrissi fault Zone in the southern margin of the Alboran Basin.

1.1.   Geological and geodynamical settings

In the southern margin of the Alboran Sea, the main structural element corresponds to the Alboran Ridge. The Alboran Ridge corresponds to a tectonic high building up since the Late-Miocene (Bourgois et al., 1992; Do Couto, 2014). The Alboran Ridge divides the Alboran Basin into three different sub-basins: the Western Alboran Basin (WAB), the South Alboran Basin (SAB), and the East Alboran Basin (EAB) (Fig. 1). Transpressive and transtensive structures associated with the Alboran Ridge and the Yusuf fault zone, respectively, as well as to several volcanic or metamorphic highs limit those sub-basins (Fig. 1). The Alboran Ridge is divided by the AIF (Fig. 1) into the South Alboran Ridge (SAR, Fig. 1), which corresponds to the submarine highs striking in the NE-SW direction (Xauen Bank, Petit Tofino Bank, Tofino bank, Ramon Margalef High, Eurofleet High, Francesc Pages High, Fig. 3) and the North Alboran Ridge (NAR; Fig 1).

Sedimentary processes shape the seafloor and control the stratigraphy. On both flanks of the Alboran Ridge, the contourite deposits produce significant thickness variations of the Quaternary depositional units, that are pinched and thinned toward the foot of the submarines highs (Juan et al., 2016). Above the Messinian Erosional Surface (MES) (Estrada et al., 2011; Garcia-Castellanos et al., 2011), the deep sedimentation in the Alboran Sea is driven by contouritic processes that also shape the seafloor since 5.33 Ma (Ercilla et al., 2016; Juan et al., 2016). Submarine erosion can occur at the moat of the contouritic systems, generally at the foot of the slopes, whereas deposition occurs at deepest locations Ma (Ercilla et al., 2016; Juan et al., 2016).

Volcanism and tectonic deformations also shaped the morphology of the Alboran Ridge. The SAR is 70 km long and corresponds to a series of faults and folds affecting the Plio-Quaternary depositional sequences (Fig. 3)(Bourgois et al., 1992; Chalouan et al., 1997; Gensous et al., 1986; Martínez-García et al., 2013; Muñoz et al., 2008; Tesson et al., 1987) and to a succession of submarine highs culminating around -110m (Fig. 3). The southern front of the SAR corresponds to the northern flank of a NE-SW syncline called the South Alboran Trough (Fig. 3). The northern front of the SAR corresponds to the Alboran Channel and the WAB (Fig. 3). The SAR marks the transition from a thinned continental crust to the north to thick continental crust to the southwest (Díaz et al., 2016). Pre-Messinian deposits are exposed at the seafloor in the core of the anticlines (Chalouan et al., 2008; Do Couto et al., 2016; Juan et al., 2016; Tesson et al., 1987). Local occurrences of volcanism in the Francesc Pagès Bank and the Ras Tarf are of Miocene age. The volcanism in the Francesc Pagès Bank is not accurately dated (Gill et al., 2004), but the lithology corresponds to basaltic rocks dated between 9.6 and 8.7 Ma in the same area by (Duggen et al., 2004). In the Ras Tarf, the volcanism ends around 9Ma (El Azzouzi et al., 2014). As evidenced by the seismic reflection data, under-compacted shales deposited during the early to mid-Miocene extensional period are present at the bottom of the sedimentary column west of the SAR (Do Couto, 2014; Do Couto et al., 2016; Soto et al., 2008).

According to Giaconia et al., (2015), since the Late-Miocene, the deformation has migrated from the Eastern Betic Margin toward the South West; the SAR might have accommodated a more recent left lateral shear than the NAR and the Carboneras Fault during the Messinian/early-Pliocene times (Fig. 1). Do Couto et al., (2016) proposed that the SAR underwent compressive deformation since 8 Ma in association with the left-lateral strike-slip of the Carboneras fault zone (Fig. 1). The SAR is a Miocene extensional structure, but E-W folds over north and south-dipping thrusts accommodate the shortening of the Alboran Basin and demonstrate a tectonic inversion (Fig. 2)(Chalouan et al., 1997). Seismic reflection profiles and well data show that the folding continued until the Quaternary in the Francesc Pagès Bank and highlight several erosion periods during Plio-Quaternary time (Galindo-Zaldivar et al., 2018; Tesson et al., 1987). Unconformities and increasing accumulation rates demonstrate three tectonic phases: a tectonic phase-1 dated from 5.33 Ma to 4.57 Ma, a tectonic phase-2 from 3.28 Ma to 2.45 Ma, and a last tectonic phase-3 between 1.81 Ma and 1.19 Ma (Martínez-García et al., 2013). More recently, it has been suggested that the uplift along the Alboran Ridge culminated around 2.45 Ma in response to compression (Martínez-García et al., 2017).

The most recent deformations involve sinistral motions in recent NNW-SSE transtensive fault network, the sinistral Al-Idrissi strike-slip fault, and the front Al-Indentation of the northern part of the Alboran Ridge (Estrada et al., 2018). The AIF is a left-

lateral shear zone crossing the NAR and the SAR at the NE tip of the Francèsc Pagès Bank. It connects to the south to the transtensive Nekor Basin (Lafosse et al., 2017), which accommodates the present-day deformation of the southern margin of Alboran (Fig. 2 and 3) (Dillon et al., 1980). Bathymetric and seismic reflection data have shown that the deformation along the AIF is accommodated through a series of sinistral NNE-SSW strike-slip faults segments (Fig. 1 and 2) (Ballesteros et al., 2008; Martínez-García et al., 2011). The AIF propagated southward during the Quaternary (Ballesteros et al., 2008; Gràcia et al., 2006; Martínez-García et al., 2011, 2013), connecting to the NNE-SSW active strike-slip faults north of the Al Hoceima region at the Boussekkour - Bokoya fault zone (d'Acremont et al., 2014; Calvert et al., 1997; Lafosse et al., 2017).

At present day, GPS velocities define an Alboran tectonic domain in between African or Iberian rigid blocks (Neres et al., 2016; Palano et al., 2013, 2015). This block is limited eastward by the TASZ and by the Yusuf Fault (Fig. 1 and 2b). East of the TASZ, the region corresponds to the SAB and the Oriental External Rif, which behave as the African block (Koulali et al., 2011; Vernant et al., 2010). GPS kinematics shows a WNW-ESE convergence rate of 4.6mm/y between Africa and Eurasia plates (Nocquet and Calais, 2004). From GPS data, the maximum present-day rates of extrusion of the Alboran tectonic domain are close to 5.5-6mm/y between the Jebha and Nekor faults (Koulali et al., 2011; Vernant et al., 2010). These geodetic data show a maximum southwestward lateral escape localized between the Nekor fault and the SAR-Jebha Fault area (Fig. 2b).

In the SAB, the AIF and the Nekor Basin are affected by significant crustal seismicity (Bezzeghoud and Buforn, 1999; Stich et al., 2005). In the area of the AIF, the earthquakes mainly occur below 30km deep (Buforn et al., 2017). In the Nekor Basin, the seismogenic depth interval is between 0 and 11km depth (Van der Woerd et al., 2014). The 1994 and 2004 earthquakes in the Al-Hoceima area reached Mw=6.3 and 5.9, respectively (Fig. 4) (Custódio et al., 2016). On January 25th, 2016, an earthquake further localized in the vicinity of the AIF zone reached Mw=6.3 (Buforn et al., 2017; Medina & Cherkaoui, 2017; Galindo-Zaldívar et al., 2018). The focal mechanisms of those three main regional earthquakes show sub-vertical nodal planes and a left lateral displacement (Fig. 4)(Bezzeghoud and Buforn, 1999; Biggs et al., 2006; Calvert et al., 1997; El Alami et al., 1998; Hatzfeld et al., 1993; Stich et al., 2005, 2006). Near the offshore Nekor Basin, close to the Moroccan coast, the NNE-SSW fault tracks identified at the seafloor in the vicinity of the epicenters can correspond to the active fault planes deduced from seismological data (d'Acremont et al., 2014; Calvert et al., 1997; Lafosse et al., 2017). In the deep basin, the January 25th 2016 earthquake sequence indicates a strike-slip style parallel to the trend of the AIF, with mainly NNE-SSW left-lateral motion (Ballesteros et al., 2008; Buforn et al., 2017; Galindo-Zaldivar et al., 2018; Martínez-García et al., 2011; Medina and Cherkaoui, 2017). The Alboran Ridge is reactivated near the AIF, as shown by several compressional focal mechanisms with NE-SW nodal planes parallel to the Alboran Ridge thrust axis, and by strike-slip focal mechanisms with a left-lateral motion (Fig. 4). In the Nekor Basin, the deformation is distributed into a normal component into the center of the basin and a left-lateral component in its boundaries (Fig. 4) (Lafosse et al., 2017). In the SAR, the style of the deformation is unclear, with focal mechanisms showing strike-slip or normal components indiscriminately (Stich et al., 2010).

2. Material and methods

2.1. Data

The data used in this study consists of multichannel seismic profiles, SPARKER and TOPAS profiles, and multibeam bathymetry. They were acquired during three oceanographic surveys (Fig. 3). The seismic reflection data were acquired with a 12-channel-streamer during the Marlboro-1 survey in 2011, as eight NNW-SSE parallel lines crossing the W-E folds of the SAR and two WSW-ENE parallel lines in the southern domain (Fig. 1, 2 and 3). During the SARAS survey in 2012 (d'Acremont et al., 2014; Lafosse et al., 2017; Rodriguez et al., 2017), were obtained SPARKER and TOPAS profiles, multibeam bathymetry and acoustic reflectivity at a 25m/pixel resolution of the deep submarine seafloor were acquired. During the MARLBORO-2 survey in 2012 (d'Acremont et al., 2014; Lafosse et al., 2017), SPARKER profiles and shallow multibeam bathymetry at a 5m/pixel resolution were acquired. The bathymetric data from the INCRISIS survey were also used (Galindo-

170   Zaldivar et al., 2018). Also, we use a Digital Elevation Model downloaded from the EMODNET data set (http://www.emodnet.eu/) to fill the missing parts of our dataset.

2.2.   Methods

We used the seismic reflection and TOPAS data interpretation to perform the tectonic mapping of the subsurface. At the seafloor, we made a visual recognition of fault scarp using the multibeam bathymetry and the curvature maps. The curvature

175   is known as a relevant parameter to track the fault offsets on 3D seismic section (e.g. Roberts, 2001) and at the seafloor (e.g., Paulatto et al., 2014). The seismic-stratigraphic analysis of the Plio-Quaternary sequences is based on the stratigraphy defined by Juan et al., (2016). The sum of the plan curvature values was made with the help of ArcGis V10.2 using the focal statistics tool to remove the smooth the noise at depths higher than -150m. The chronology of the seismic stratigraphic boundaries was defined based on an age calibration on data from scientific wells DSDP 121 and ODP 976, 977, 978, and 979 (Fig. 1 and 5)

180   (Ercilla et al., 2016; Juan et al., 2016). Using the velocity analysis for the ODP well 976 (Soto et al., 2012), we consider an average P-wave velocity of 1750m/s for the Plio-Quaternary pelagic sedimentation. We propose seismic stratigraphy and sequential stratigraphy interpretations of depositional units based on the nomenclature and general principles presented in the literature (Catuneanu, 2007; Catuneanu et al., 2011). All seismic lines shown in the present manuscript are presented without interpretation in the supplementary materials (Figures S1 to S8, Supplementary materials).

185   ## 3.   Results

3.1.   Plio-Quaternary seismic stratigraphy

The Plio-Quaternary sedimentary sequence of the southern margin of the Alboran Sea has been divided into three Pliocene (Pl1, Pl2, and Pl3) and four Quaternary (Qt1 to Qt4) seismic units, based on the Juan et al. (2016) seismic stratigraphy (Fig. 5). These units are limited at the bottom by discontinuity surfaces, M, P0, and P1 for the Pliocene units, and BQD, Q0 to Q2,

190   for the Quaternary units. Boundaries represent discontinuity surfaces mostly defined by onlap and erosive surfaces; locally, downlap surfaces are identified (Fig. 6 and 7). Sub-parallel, parallel, oblique, and wavy stratified reflections characterize the Plio-Quaternary units. Pl1, Pl2, and Pl3 units are pinching toward the structural highs and evidence aggrading wedges geometries. The Quaternary seismic units (QT1 to QT4) show an aggradational geometry and are confined to the foot of the folds where they pinch on the older tilted Pliocene deposits (Fig. 6 and 7)(Juan et al., 2016). Contouritic deposits and associated

195   sedimentary features, MTDs and volcanic deposits constitute the Plio-Quaternary units. The plastered drifts type is dominant and contributes to cover the structural highs (Juan et al., 2016). In seismic reflection, truncation at the foot of topographic high corresponds to contourite moats and channels (Fig. 7). Sediments present local intercalations of lenticular chaotic or transparent facies interpreted as mass-flow deposits and correspond to scars on the bathymetry (Fig. 3)(Rodriguez et al., 2017). Regarding the volcanic deposits, two buried volcanic edifices are identified on seismic reflection: the Big Al-Idrissi Volcano (Fig. 3, 8

200   and 11), and the Small Al-Idrissi Volcano (Fig. 6, 9 and 11). Acoustically, they correspond to a seismic facies of poorly continuous high amplitude reflectors (Fig. 9). Pliocene to Quaternary reflectors onlaps on these seismic units (Fig. 8 and 9). The Big Al-Idrissi Volcano corresponds to a conic structure located to the North of the Ras Tarf (Fig. 8) that has been interpreted as an N-S volcanic ridge in Bourgois et al. (1992). The top of this seismic body merges with the M-Reflector (Fig. 8). Plio-Quaternary seismic units showing prograding to aggrading sigmoid reflectors characterizes the growth of a continental

205   shelf above the M reflector burying this volcano (Fig. 8). On the west side of this seamount, the trajectory of the offlap breaks is concave up, indicating that the rate of progradation decreases progressively with time. Reflectors onlaps terminations on the bottomsets and foresets of the prograding seismic units mark the beginning of a retrogradation after 1.81 Ma (Fig. 8). West dipping normal faults offset the depositional unit of prograding sigmoid reflectors (Fig. 8). Those normal faults correspond to scarps at the seafloor (Fig. 8 and 11). Toward the top of the sequence, the bottomsets of the late-Pleistocene Moroccan shelf

offshore of the Ras Tarf corresponds to a unit of flat-lying reflectors (Fig. 8). The flat top of the Big Al-Idrissi volcano culminates at an approximate depth of 150-200 m below the present-day sea level and corresponds to a toplap surface (Fig. 8). It the South Alboran Through, the Small Al-Idrissi volcano shows a roughly NNE-SSW spatial extent and a 4-5 km wide conic structure (Fig. 9, 10 and 11). This seismic body intercalated within the Pl1 seismic unit (Fig. 9) corresponds to rounded high at the seafloor narrow submarine high (Fig. 11), which pinches abruptly toward the West (Fig. 9). The top of the Pl1 seismic unit rests unconformably on this seismic body indicating an early-Pliocene age (Fig. 9). In the Francesc Pagès Bank, a seismic body with similar facies is present at the core of an NNE-SSW striking anticline (Fig. 6), truncated by the M reflector (Fig. 6). The stratigraphic architecture of the shelf north of the Nekor Basin records an early-Quaternary regression (Fig. 12). We follow the Q1 surface northeastward toward the top of the submerged shelf surrounding the Big Al-Idrissi Volcano (Fig. 8). The Q0 reflector corresponds to an unconformity at the bottom of prograding oblique reflectors. This depositional unit displays the geometry of continental shelf deposits. The most distal offlap break shows the maximum extent of the continental shelf north of the Nekor Basin during the Pleistocene. It indicates that the retrogradation of the shoreline starts before 1.12 Ma and after 1.81Ma (Q1 reflector, Fig. 12). The most distal offlap break near Al-Hoceima is located around 312±30 mstwt, corresponding to a depth of 188±5 m below sea level (Fig. 12). In the distal part of the shelf, we interpret a seismic body of poorly continuous wavy reflectors deposited above an erosional surface as a local mass transport complex, which could mark an early Quaternary destabilization of the shelf.

3.2. Evidence and style of the compressive deformation

The seismic stratigraphy shows that the Plio Quaternary sequence records two principal phases of deformation. Folds and faults along the Alboran Ridge demonstrate a Pliocene compressive phase. On the Moroccan shelf, the stratigraphic pattern indicates a regressive trend. The second phase is younger and corresponds to the developing activity of strike-slip and normal faults, which control the local transgressions of the Moroccan shelf.

3.2.1. Folded structures of the South Alboran Ridge (SAR)

Bounded by the WAB and the South Alboran Trough, the SAR region corresponds to an N065° 80km long folded area (Fig. 6). The shortening in the SAR is distributed from east to west over the 10 to 25 km wide SAR structure, composed of a series of two to four 4 km-wavelength anticlines (Figs. 6 and 10). Northward-verging anticlines characterize the northern front of deformation (Fig. 6). In the eastern part of the SAR, the Francesc Pagès and the Eurofleet Highs correspond to pinched anticlines, in a 10 km narrow fold, over south-verging thrusts (MAB16 and 14; Fig. 6). Several southward and northward dipping blind thrusts affect the M reflector (Fig. 6). From East to West and above the thrusts faults, a series of anticlines and synclines draw a sigmoidal pattern (Fig. 10). Azimuths of the hinge axis tend toward the E-W direction at the center of the folds and toward an N065° direction toward the tips of the folds, therefore demonstrating left lateral deflections of their hinge axis and overall sigmoidal shape (Fig. 6 and 10). The orientation of the most western tip of the SAR changes from NE-SW to E-W (Fig. 6).

Below the M surface, truncated Miocene seismic units show local folding (Fig. 6f)(Do Couto et al., 2016). It indicates that a shortening occurred in the SAR before the Messinian Salinity Crisis (MSC). The lateral and vertical strata pattern of the Plio-Quaternary units shows that the shortening occurs mostly during the Pliocene. Along the northern flank of the SAR, tectonic tilting and the growth of the contouritic drift deposits produce P0 to BQD unconformities (Fig. 7). The intra-Pliocene unconformities, the tilting of the Pliocene units, and the aggradation of Quaternary contouritic deposits on top of the sedimentary sequence indicate a compressive deformation ending around the early Quaternary (Fig. 6 and 9). Within the Pliocene sequence, the folding appears to be progressive and diachronic from East to West. At the foot of the Francesc Pagès Bank, P1 reflectors are unconformably lying on the P0 reflector (Fig. 7a). At the foot of the Ramon Margalef High, Pliocene reflectors older than P1 show a more even geometry with constant thickness, where P0 is a conformable surface (Fig. 7b).

Parallel to the SAR, the South Alboran Trough corresponds to a syncline that narrows from East to West (Fig. 6). Its northern flank is steeper than the southern one (Fig. 6). The local variations of thicknesses reveal the non-cylindrical folding of the syncline (Fig. 6 and 10). The progressive tilt of the QT1 to QT4 units and internal growth strata reveal a more continuous Quaternary to Pleistocene folding of the South Alboran Trough (Fig. 6, and 9) near the Al-Idrissi fault zone (Fig. 9). It indicates that local folding persists during the Quaternary.

3.2.2. The Al-Idrissi fault zone

At present day, the AIF is an NNE-SSW fault zone composed of several segments following the older structural trend (Fig. 11). Crossing the eastern end of the Francesc Pagès Bank and the western end of the NAR, it forms a positive flower structure distinct from the Pliocene thrust of the Alboran Ridge (Fig. 13). The flower structure corresponds to a compressional bend of the AIF affects the most-recent Quaternary sediments (Fig. 11 and 13), whereas Pliocene thrusts appear to be abandoned during the Quaternary (Fig. 13). The depth of the Messinian unconformity at the western tip of the Alboran Ridge is lower than at the Francesc Pages Bank (Fig. 10), indicating different uplift/subsidence rates from either part of the AIF. The location of the compressional bend is highlighted at present-day by the cluster of compressive focal mechanisms (Fig. 4) (Stich et al., 2010). At the southern tip of the AIF, NNE-SSW fault segments affect present-day deposits and correspond to splay faults distributing the deformation (Fig. 9 and 11). Below the volcanic facies, poor acoustic penetration prohibits the interpretation of tectonic structures (Fig. 9). At the seafloor, the fault tracks are clear toward the southwest where they offset the Small Al-Idrissi volcano and link to the Bokoya fault (Fig. 10 and 11).

Affecting the SAR, N145° striking lineaments at the seafloor correspond to sub-vertical normal faults affecting the sub-surface sediments (Fig. 11 and 14). At the northern flank of the SAR, the fault network describes a 10-12km wide shear zone (Fig. 14). The recognition of pockmarks at the seafloor and signal attenuation near the faults on the seismic reflection data, which suggests fluid seepages along active faults (Fig. 14) (Judd and Hovland, 2009). Northward, the faults disappear at the seafloor under the present-day depositional part of the contourite. In the subsurface, they affect Q1 and Q2 surfaces demonstrating late Pleistocene activity (Fig. 14b). Southward, we lost the fault tracks against the hinge axis of the Francesc Pagès fold. At the southwestern flank of the Francesc Pagès fold, similar NW-SE striking faults affect the seafloor (Fig. 11a). These N145° lineaments observed at the surface correspond to the normal faults pointed in red on the TOPAS profile (Fig. 6b), that uplift the western block of the fault wall. Despite reduced expression at the seafloor, this fault zone continues southeast, where it affects the whole Plio-Quaternary sequence (Fig. 9). Along the AIF, the vertical offset of the P1 surface is around 100m (Fig. 9). Between the N145° faults and the AIF, several fault segments affect the subsurface highlighting the distributed deformation that occurs between the N145° faults and the AIF with a higher apparent vertical offset along the AIF (Fig. 9).

4. Discussion

Our results show at least two phases of tectonic activity from the Early-Pliocene to the present day and that the Al-Idrissi Fault zone is a new feature (<1.8Ma) profoundly affecting the regional deformation. The first phase of compressive deformation starts probably during the Tortonian and ends during the early Quaternary, with the possible local occurrence of volcanism and a strike-slip component. The second phase starts clearly after 1.8 Ma and continues today. It corresponds to a strike-slip phase with an important extensional component. Both phases evidence the overall oblique convergence and essential control of deep structures, which we detail thereafter.

4.1. Mio-Pliocene to Early Quaternary strain partitioning

The first tectonic phase occurred from the Mio-Pliocene to the Early Quaternary. The overall geometry of the SAR deformation shows the development of imbricated folds distributed throughout a left-lateral shear zone along N065° striking thrust faults

290   (Fig. 6). The change of stacking pattern of the Pliocene deposits along the folds suggests a diachronous growth during the Pliocene with the lateral variation of the uplift rates (Fig. 6 and 7). The aggradation of contourites at the foot of the SAR indicates a relative quiescence of the folding during the Quaternary after 2.6 Ma (Juan et al., 2016).

Mio-Pliocene shortening is locally contemporaneous of volcanism. The lateral continuity of the highly reflective facies from west to east suggests that the Small Al-Idrissi and the Big Al-Idrissi volcanoes are a structure that are offset by local extensional
295   faults during the Pleistocene (Fig. 8 and 10). This highly reflective material triggers the acoustic masking of the reflections below (Fig. 9), as observed in debris-avalanche deposits elsewhere (Le Friant et al., 2002, 2009). The intercalation of this volcanic material toward the top of the Pl1 unit indicates that the Small Al-Idrissi Volcano could be older than 4.5 Ma but younger than 5.33 Ma (Fig. 9). The NE-SW distribution of the volcanic material suggests a syn-folding infill of the N065° striking syncline axis (Fig. 10). The local volcanism can be contemporaneous to the volcanic activity occurring to the North
300   of the Alboran Ridge, dated between 5 Ma and 4.4 Ma (Duggen et al., 2008). This volcanism generally shows high K content and occurs above the thinned continental lithosphere (Duggen et al., 2008). It could also be the product of decompression partial melting after the Messinian Salinity Crisis, as proposed for the onshore Pliocene Moroccan volcano by Sternai et al., (2017).

The sigmoid folds in the SAR draw a rhombic pattern (Fig. 10). Within the N065° trend of the SAR, their overall E-W strikes
305   evidence left lateral transpression during the Pliocene. NE-SW thrust faults distribute the deformation and probably accommodate the strike-slip motion during the Pliocene. The distribution of the deformation into left-lateral motion and shortening reflects the onset of an oblique direction of shortening relatively from NE—SW basement faults (i.e., between the Nekor and Jebha Fault and the Alboran Ridge). The left-lateral shear component of the deformation of the Alboran domain implies vertical axis rotation of the basement faults (Fig. 15a to 15c), as demonstrated elsewhere (Koyi et al., 2016; Tadayon
310   et al., 2018). It suggests that the deformation progressively switches from left-lateral transpressive to compressive strike-slip (Fig. 15a and 15b). Vertical axis rotations favor a progressive change from transpressive to more purely compressive.

The development of oblique faults and thickness variation in the sedimentary cover, which results in non-cylindrical thrust wedges, lateral escape of frontal thrust sheets and vertical-axis block rotations demonstrate the influence of a viscous layer at the base of the sedimentary covers, as demonstrated from analog modeling (Storti et al., 2007). In the SAR, such a weak layer
315   can correspond to the early-Miocene under-compacted shales at the bottom of the sedimentary covers (Soto et al., 2008, 2012). Such weak layer can explain why the deformation is distributed in the SAR, whereas it appears to be more localized in the NAR.

The Pliocene oblique compression offshore is equivalent to transpressive tectonic in the Rif (Table 1). The Nekor fault and the Jebha Fault accommodate a distributed deformation onshore, and a transpressive deformation is recorded offshore around the
320   SAR (Fig. 15a). The passive infilling of paleo-rias indicates relatively low vertical motion (Romagny et al., 2014). After 3.8 Ma, a transition from compression to radial extension (Benmakhlouf et al., 2012) causes NE-SW normal faulting and tectonic tilting of the Moroccan margin (Fig. 15b)(Romagny et al., 2014). Toward the south-east, the Nekor fault has acted as a transpressive fault zone accommodating the shortening (Ait Brahim et al., 2002; Aït Brahim and Chotin, 1990). The offshore extensional faults prolonging the Nekor fault are sealed offshore by Pliocene deposits and were inverted as blind thrust faults
325   during the Plio-Quaternary (Watts et al., 1993). In the external Rif, in southwest continuity of the Nekor Fault, field studies demonstrate NE-SW compression (Roldán et al., 2014). Interpretations of 2D seismic reflection lines indicate thick-skin tectonic from Tortonian-early Messinian to Pliocene times, causing the uplift of intramountainous basins around the Nekor fault (Fig. 15a)(Capella et al., 2016).

4.2. Quaternary to present-day strain partitioning

4.2.1. Evidences of Quaternary tectonic subsidence

In contrast to the SAR region, in the NAR, the recorded uplift increases through time until it reaches a maximum around 2.45 Ma, with a clear pop-up structure (Martínez-García et al., 2017). It could be linked to the incipient activity of the AIF and suggests that the AIF progressively decouples the deformation between the NAR and the SAR from 2.6 – 2.45 Ma (Table 1). Before 1.8Ma, basinward motion of the shelf along the Big – Al Idrissi volcano and normal regressive geometry of the shelf wedges argue for progradation driven by sediment supply. It can indicate positive accommodation at the coastline (Catuneanu et al., 2011). In the overall regressive trend, syncline formation can create accommodation space.

After 1.8 Ma, the later Pleistocene transgression is linked to the normal faulting along N-S faults (Fig. 8 and 12). Including the onshore Trougout and Boudinar faults, we interpret the N-S fault network as an *en-echelon* right stepping set of normal faults (Fig. 10 and 15). Focal mechanism and microstructural studies demonstrate that this fault network is likely to be active with a normal sinistral component at present-day (Fig. 4) (Poujol et al., 2014). The local stratigraphy recorded the start of the activity of this tectonic structure. The depth of the Pleistocene offlap breaks and the geometry of the shelves indicate evident tectonic subsidence during the Pleistocene contemporaneous with the northward tilting of the margin (Ammar et al., 2007). The Moroccan shelf underwent a local transgression and flooding characterized by the building of transgressive wedges on top of a prograding clinoforms (Fig. 7 and 12). The retrogradation of the shoreline starts between 1.8 Ma and 1.12 Ma in the Nekor Basin and the Big Al-Idrissi volcano (Table 1). The depths of the offlap breaks are significantly lower than the maximum depths reached by the sea-level falls at Gibraltar during the Quaternary (Fig. 6 and 7) (Rohling et al. 2014) and proves the tectonic subsidence.

4.2.2. Evolution and localization of the Al-Idrissi fault zone

The beginning of the transgression of the shelf around the Big Al-Idrissi volcano and the Nekor Basin is approximately synchronous of the last shortening event along the NAR (1.8 to 1.12 Ma)(Table 1). The AIF has progressively propagated southward, activating the N-S right-stepping normal fault linking from the AIF to Boudinar and Nekor Basins during the Quaternary (Fig. 15b). Since *ca*. 1.8 Ma-1.12 Ma, the transgression of the shelf of the Big Al-Idrissi volcano and the subsidence of the Nekor Basin indicated localization of the deformation on a releasing bend activating N-S faults. The compressional bend in the northern part of the AIF affect the seafloor and is activated during the recent seismic crisis (Buforn et al., 2017; Galindo-Zaldívar et al., 2015). In the eastern part of the SAR, N145° normal faults are active with an orientation similar to the N140° normal faults accommodating the late-Pleistocene extension in the Nekor Basin (Fig. 10, 11 and 14) (Lafosse et al., 2017). From the local direction of the maximum horizontal stress field and focal mechanisms (Fig. 2b and 4) (Neres et al., 2016), the fault zone is transtensive with a right-lateral motion. We can regard this fault zone as an antithetic or extensional structure accommodating the present-day left-lateral motion along the AIF, or extensional structures related to the southern fault tip in the horsetail splay (Fig. 15c). The apparent low lateral offset and the localization of the deformation on the strike-slip Boussekkour-Bokoya fault zone after 0.8 Ma suggest that the localization of the deformation along the AIF is a recent feature (Fig. 15c) (Lafosse et al. 2017). In this context, the normal faults are equivalent to antithetic faults within a horsetail splay, that connect to the Trougout Fault and the Nekor faults (Fig. 15b). Such structures grow probably through a mechanism of relay ramp, like the one proposed in other strike-slip contexts such as the Paleogene Bowey Basin (Peacock and Sanderson, 1995). It denotes a progressive localization of the deformation along the AIF and westward migration of the deformation as proposed in Lafosse et al., 2017 and Galindo-Zaldivar et al., 2018 (Fig. 15c).

The inception of the southern Al-Idrissi fault zone after 1.8Ma is coherent with similar ages found for the inception of strike-slip tectonics in the Djibouti Plateau area where the set of conjugated strike-slip Al-Idrissi and Averroes faults is dated around 1 - 1.1Ma (Fig. 1 and Table 1)(Estrada et al., 2018; Gràcia et al., 2019; Perea et al., 2018). The AIF decouples the deformation

370 in the SAR and the NAR and acts as a transfer fault accommodating the shortening north of the Alboran Ridge (Estrada et al., 2018) and the Rifian extrusion along the Nekor fault. The localization of the deformation along the AIF could be controlled by a Miocene pre-existing structure, as proposed in Martínez-García et al., (2017). At a crustal-scale, geophysical studies show a ~20-30km crustal thickness variation at the Al Hoceima region (Diaz et al., 2016), which can contribute to the localization of the deformation. The contrasted crustal thickness origins either in a Miocene oblique collision (Booth-Rea et al., 2012),

375 lower crust doming during the Miocene transtension (Le Pourhiet et al., 2014), or lower crust removal associated to delamination processes (Bezada et al., 2014; Petit et al., 2015). The localization of the deformation on crustal heterogeneity has been evidenced in numerical models, for example, in the cratonic lithosphere (Burov et al., 1998). It follows that the localization of deformation along the AIF evidences the control of the crustal heterogeneities.

4.3.   Evolution of the southeastern limit of the Betico-Rifian tectonic domain

380 The late Miocene-early Pliocene period in the Rif Belt matches the uplift of the Miocene intramountainous basin along the Nekor fault under a transpressional tectonic regime (Fig. 15a and table 1). The uplift of those basins corresponds to the change from thin-skin to thick-skin deformation in the external Rif during the inversion of the deep Mesozoic extensional structures (Capella et al., 2016; Martínez-García et al., 2017) and during the transpressive deformation in the Temsamane units (Fig. 1)(Booth-Rea et al., 2012). It suggests a progressive mechanical coupling between the African Margin and the Alboran

385 Domain, locking the Nekor fault in its eastern segment (Fig. 15). In the External Rif, paleo-magnetic data evidence at least 20° of counter-clockwise rotation since the upper Miocene (Crespo-Blanc et al., 2016; Platt et al., 2003). Progressive vertical axis rotation associated with the shortening of the Alboran Basin decreases the left lateral shear, and increase the compressive deformation along the Alboran Ridge (Fig 15b). Eventually, the deformation has localized on the AIF during the early Quaternary decoupling the deformation between the NAR and the SAR with a developing transtensive mode from 1.81 Ma

390 (Fig. 15c). It induces a change of strain partitioning along the TASZ illustrated by the transition from a Pliocene left-lateral shearing and folding of the SAR to a transtensive Quaternary deformation localized on the AIF and the Nekor Basin (Fig. 15). Changes of tectonic style in the Alboran Basin have been related to changes in the direction of far-field forces (Martínez-García et al., 2013). However, since 5 Ma, the direction of Africa Eurasia convergence remains constant (DeMets et al. 2015). In an absolute reference frame, the direction of convergence between Africa and Eurasia is NNE-SSW, producing 15km of

395 shortening since 8Ma (Spakman et al., 2018). From GPS measurements and from present-day stress and strain modelling, the Alboran tectonic domain can be considered as a tectonic domain undergoing a clockwise rotation of 1.17°/Ma (Palano et al., 2013, 2015). This value has the same order of magnitude to the domino model from Meghraoui and Pondrelli (2013) of a tectonic block undergoing a long term clockwise rotation of 2.24˚/Ma to 3.9˚/Ma.

In the Alboran Basin, the TASZ must rotate as well to accommodate the convergence and block rotation (Fig. 15). It follows

400 that during the Pliocene and a part of the Pleistocene, the direction of far-field forces is oblique to principal fault planes of the Alboran ridge. Because of the vertical axis rotation, the obliquity decreases progressively, which leads to the present-day more orthogonal compression along the NAR (Fig. 2b and 15)(Cunha et al., 2012; Neres et al., 2016) and the inversion of the Alboran Basin and the Algerian Margin (Derder et al., 2013; Hamai et al., 2015; Martínez-García et al., 2017). Therefore, the evolution of the deformation in the Alboran Ridge represents the expected evolution of transpressive structures under a constant

405 shortening and indentation of the African lithosphere (Fig. 15). Block rotations and transpressive folds propagation followed by transtensive deformation during the inception of the AIF represent successive steps within the tectonic inversion of the Alboran Domain since 8Ma.

In this framework, normal strike-slip behaviour observed to the north of the NAR (Fig. 1)(Giaconia et al., 2015; Gràcia et al., 2012; Grevemeyer et al., 2015; Palomino et al., 2011) goes a step further in the sense of an indentation of the Africa plate into

410 the Alboran tectonic domain (Fig. 2)(Estrada et al., 2018; Palano et al., 2015). This indentation is accommodated through the left-lateral AIF and the right-lateral Averroes Yusuf fault zone (Fig. 1 and 15) in a similar way than the Palomares fault zone

transferring the orthogonal shortening of the Iberian margin toward the Carboneras fault zone and the Central Alboran Sea (Estrada et al., 2018; Giaconia et al., 2015). In the SAR and the Nekor Basin, the present-day deformation under the transtensional regime (NNW-SSE to N-S extensional network and NNE-SSW strike-slip faults; Fig. 4 and 15) is limited to the

415   east by the Al-Idrissi fault. The deformation in the NAR is on the contrary clearly compressive (Estrada et al., 2018; Martínez-García et al., 2017) and the geodetic data indicates similar displacements in the EAB and in the Rifian units east of the Boudinar Basin (Koulali et al., 2011; Vernant et al., 2010). Such difference of behavior suggests that the AIF may represent the present-day plate boundary between Africa and Alboran Domain.

5.   Conclusion

420   This study focuses on the tectonic evolution of the southern margin of the Alboran Sea during the Plio-Quaternary period, and particularly the distinct structural evolutions and interactions of the AIF and the AR, and the mechanisms associated to their formation. The analysis of the seismic stratigraphy and the comparison between onshore and offshore tectonic structures leads to the following tectonic framework:

(1) The TASZ, and in particular the Alboran Ridge, localizes the deformation between the Miocene and the early
425   Quaternary. Its orientation favors a strike-slip movement during its oblique shortening. The rhombic folded structures of the SAR illustrate a significant left-lateral displacement during the Pliocene. Consequently, during the Pliocene, the SAR accommodates the strain partitioning between left-lateral strike-slip and shortening.

(2) Under the indentation of African lithosphere, vertical-axis block rotations, which lead to a progressive compression on the Alboran Ridge and a younger activation under left lateral transtension along the AIF. The subsidence of both
430   the Nekor Basin and the Big Al-Idrissi volcano demonstrate the start of the transtensive deformation between 1.8 Ma and 1.12.

(3) The SAR undergoes transpression whereas further east tectonic inversion of the Algerian and Iberian margin occurs. The area between the SAR and the Nekor fault is progressively extruded, whereas east of the Al-Idrissi fault, the African lithosphere indents the Alboran tectonic domain. The AIF transfers this indentation to the Nekor Basin, which
435   accommodates the present-day westward extrusion of the Rif and represents an incipient plate boundary since 1.8 Ma.

Our findings demonstrate that at the scale of a basin, strike-slip shear zones evolve in response to far-field forces but also in response to the local evolution of the fracture zone. This evolution is fast and achieved in less than 2 Ma. Further researches are needed to understand better what drives the timing and the evolution of such large scale-strike slip structures.

6.   Author contribution

440

Manfred Lafosse wrote the paper and conducted the study.

Elia d'Acremont and Christian Gorini lead the oceanic surveys MARLBORO-1, 2 and SARAS. They contributed to study and to the redaction of the present paper.

Alain Rabaute contributed to the data acquisition and processing and to the redaction of the present paper.

445   Ferran Estrada contributed to the data acquisition and processing.

Martin Jollivet-Castelot contributed to the stratigraphic interpretation.

Juan Tomas Vazquez contributed to the data acquisition and processing.

Jesus Galindo-Zaldivar and Gemma Ercilla contributed to the data acquisition and processing. They are the PI of the INCRISIS survey. Gemma Ercilla also contributed to the stratigraphic correlations and interpretations.

450   Belen Alonso contributed to the stratigraphic correlations and interpretations.

Abdellah Ammar contributed to the data acquisition.

7. Acknowledgement

We thank the members of the SARAS and Marlboro cruises in 2011 and 2012. We also thank Dr. Lodolo and Prof Déverchère for their helpful comments. This work was funded by the French program Actions Marges, the EUROFLEETS program (FP7/2007-2013; n°228344), project FICTS-2011-03-01. The French program ANR- 17-CE03-0004 also supported this work. Seismic reflection data were processed using the Seismic UNIX SU and Geovecteur software. The processed seismic data were interpreted using Kingdom IHS Suite©software. This work also benefited from the Fauces Project (Ref CTM2015-65461-C2-R; MINCIU/FEDER) financed by "Ministerio de Economía y Competitividad y al Fondo Europeo de Desarrollo Regional" (FEDER).

8. Competing interests

"The authors declare that they have no conflict of interest."

9. Tables

Age (Ma) / Epoch	Rifian Units		South Al Idrissi Fault zone			Alboran Ridge				North Al Idrissi Fault zone			East Alboran Basin	
	Central Rif *Ref: (1, 2)*	Onshore Nekor Fault + External Rif Units (3, 5)	Bokoya Fault zone (*,4)	Nekor Basin (*, 4)	Big Idrissi Volcano / NS faults (*, 4, 5)	N145° fault zone (*, 6)	SAR (*, 7)	NAR (8, 9)	AIFZ Central segments (*, 8, 9, 10)	Djibouti Plateau (10)	Adra fault zone (10)	Averoes fault (10, 11)	Yusuf fault (8, 9)	Abubacer Ridge (12)
Pleistocene Middle	↓ (?)						Local compressionnal reactivation		↓ (?)		↓ (?)	strike - Slip		
Pleistocene Calabrian					AIF early propagation ↓ (?)			Pulse 3						
Pliocene Gelasian	↑ (?) Uplift + Radial extension							Pulse 2	Early (re)-activation of the AIF ?				Compression Transtension	Compression
Pliocene Piacenzian		↑ (?) Compression and uplift of the intra-moun- tainous Rifian basins + anticlockwise rotation			Boudinar Basin emersion									
Pliocene Zanclean					Boudinar Basin max transgression			Pulse 1				NW -SE folding ↓(?)	strike - Slip	

Table 1. Synthesis of the tectonic events in the Alboran Basin, and the Rif from the literature and the present study. *, this study; (1), Benmakhlouf et al., (2012) ; (2), Romagny et al., (2014) ; (3) Aït Brahim and Chotin, (1990), (4), Lafosse et al., (2017); (5), Azdimousa et al., (2006); (6), Galindo-Zaldivar et al., (2018); (7) Juan et al., (2016); (8) Martínez-García et al., (2013) ; (9), Martínez-García et al., (2017); (10), Gràcia et al., (2019); (11), Perea et al., (2018); (12) Giaconia et al., (2015). The main tectonic events are in green. Green arrows and question marks figure the age uncertainties of the main tectonic events.

10. Bibliography

d'Acremont, E., Gutscher, M.-A., Rabaute, A., Mercier de Lépinay, B., Lafosse, M., Poort, J., Ammar, A., Tahayt, A., Le Roy, P., Smit, J., Do Couto, D., Cancouët, R., Prunier, C., Ercilla, G. and Gorini, C.: High-resolution imagery of active faulting offshore Al Hoceima, Northern Morocco, Tectonophysics, doi:10.1016/j.tecto.2014.06.008, 2014.

Aït Brahim, L. and Chotin, P.: Oriental Moroccan Neogene volcanism and strike-slip faulting, Journal of African Earth Sciences, 11(3/4), 273–280, doi:https://doi.org/10.1016/0899-5362(90)90005-Y, 1990.

Ait Brahim, L., Chotin, P., Hinaj, S., Abdelouafi, A., El Adraoui, A., Nakcha, C., Dhont, D., Charroud, M., Sossey Alaoui, F., Amrhar, M., Bouaza, A., Tabyaoui, H. and Chaouni, A.: Paleostress evolution in the Moroccan African margin from Triassic to Present, Tectonophysics, 357(1–4), 187–205, doi:10.1016/S0040-1951(02)00368-2, 2002.

Alvarez-Marrón, J. and others: Pliocene to Holocene structure of the eastern Alboran Sea (western Mediterranean), in Proceedings of the Ocean Drilling Program-Scientific Results, vol. 161, pp. 345–355. [online] Available from: http://digital.csic.es/handle/10261/17611 (Accessed 19 June 2014), 1999.

Ammar, A., Mauffret, A., Gorini, C. and Jabour, H.: The tectonic structure of the Alboran Margin of Morocco, Revista de la Sociedad Geológica de España, 20(3–4), 247–271, 2007.

Ballesteros, M., Rivera, J., Muñoz, A., Muñoz-Martín, A., Acosta, J., Carbó, A. and Uchupi, E.: Alboran Basin, southern Spain—Part II: Neogene tectonic implications for the orogenic float model, Marine and Petroleum Geology, 25(1), 75–101, 485 doi:10.1016/j.marpetgeo.2007.05.004, 2008.

Benmakhlouf, M., Galindo-Zaldívar, J., Chalouan, A., Sanz de Galdeano, C., Ahmamou, M. and López-Garrido, A. C.: Inversion of transfer faults: The Jebha–Chrafate fault (Rif, Morocco), Journal of African Earth Sciences, 73–74, 33–43, doi:10.1016/j.jafrearsci.2012.07.003, 2012.

Bezada, M. J., Humphreys, E. D., Toomey, D. R., Harnafi, M., Dávila, J. M. and Gallart, J.: Evidence for slab rollback in 490 westernmost Mediterranean from improved upper mantle imaging, Earth and Planetary Science Letters, 368, 51–60, doi:10.1016/j.epsl.2013.02.024, 2013.

Bezada, M. J., Humphreys, E. D., Davila, J. M., Carbonell, R., Harnafi, M., Palomeras, I. and Levander, A.: Piecewise delamination of Moroccan lithosphere from beneath the Atlas Mountains, Geochemistry, Geophysics, Geosystems, 15(4), 975–985, doi:10.1002/2013GC005059, 2014.

495 Bezzeghoud, M. and Buforn, E.: Source parameters of the 1992 Melilla (Spain, MW= 4.8), 1994 Alhoceima (Morocco, MW= 5.8), and 1994 Mascara (Algeria, MW= 5.7) earthquakes and seismotectonic implications, Bulletin of the Seismological Society of America, 89(2), 359–372, 1999.

Biggs, J., Bergman, E., Emmerson, B., Funning, G. J., Jackson, J., Parsons, B. and Wright, T. J.: Fault identification for buried strike-slip earthquakes using InSAR: The 1994 and 2004 Al Hoceima, Morocco earthquakes, Geophysical Journal 500 International, 166(3), 1347–1362, doi:10.1111/j.1365-246X.2006.03071.x, 2006.

Booth-Rea, G., Jabaloy-Sánchez, A., Azdimousa, A., Asebriy, L., Vílchez, M. V. and Martínez-Martínez, J. M.: Upper-crustal extension during oblique collision: the Temsamane extensional detachment (eastern Rif, Morocco): The Temsamane extensional detachment (eastern Rif, Morocco), Terra Nova, 24(6), 505–512, doi:10.1111/j.1365-3121.2012.01089.x, 2012.

Bourgois, J., Mauffret, A., Ammar, A. and Demnati, A.: Multichannel seismic data imaging of inversion tectonics of the 505 Alboran Ridge (Western Mediterranean Sea), Geo-Marine Letters, 12(2–3), 117–122, 1992.

Buforn, E., Pro, C., Sanz de Galdeano, C., Cantavella, J. V., Cesca, S., Caldeira, B., Udías, A. and Mattesini, M.: The 2016 south Alboran earthquake (M w = 6.4): A reactivation of the Ibero-Maghrebian region?, Tectonophysics, 712–713, 704–715, doi:10.1016/j.tecto.2017.06.033, 2017.

Burov, E., Jaupart, C. and Mareschal, J. C.: Large-scale crustal heterogeneities and lithospheric strength in cratons, Earth and 510 Planetary Science Letters, 164(1–2), 205–219, doi:10.1016/S0012-821X(98)00205-2, 1998.

Calvert, A., Gomez, F., Seber, D., Barazangi, M., Jabour, N., Ibenbrahim, A. and Demnati, A.: An integrated geophysical investigation of recent seismicity in the Al-Hoceima region of North Morocco, Bulletin of the Seismological Society of America, 87(3), 637–651, 1997.

Capella, W., Matenco, L., Dmitrieva, E., Roest, W. M. J., Hessels, S., Hssain, M., Chakor-Alami, A., Sierro, F. J. and 515 Krijgsman, W.: Thick-skinned tectonics closing the Rifian Corridor, Tectonophysics, doi:10.1016/j.tecto.2016.09.028, 2016.

Catuneanu, O.: Principles of sequence stratigraphy, 1. ed., reprinted., Elsevier, Amsterdam., 2007.

Catuneanu, O., Galloway, W. E., Kendall, C. G. St. C., Miall, A. D., Posamentier, H. W., Strasser, A. and Tucker, M. E.: Sequence Stratigraphy: Methodology and Nomenclature, Newsletters on Stratigraphy, 44(3), 173–245, doi:10.1127/0078-0421/2011/0011, 2011.

520 Chalouan, A., Saji, R., Michard, A., Bally and W., A.: Neogene tectonic evolution of the southwestern Alboran basin as inferred from seismic data off Morocco, Aapg Bulletin-American Association of Petroleum Geologists, 81, 1161–1184, 1997.

Chalouan, A., Michard, A., El Kadiri, K., Negro, F., Frizon de Lamotte, D., Soto, J. I. and Saddiqi, O.: The Rif Belt, in Continental evolution: the geology of Morocco, pp. 203–302., 2008.

Comas, M. C., Platt, J. P., Soto, J. I. and Watts, A. B.: The origin and Tectonic History of the Alboran Basin: Insights from 525 Leg 161 Results, Proceedings of the Ocean Drilling Program Scientific Results, 161, 555–580, 1999.

Crespo-Blanc, A., Comas, M. and Balanyá, J. C.: Clues for a Tortonian reconstruction of the Gibraltar Arc: Structural pattern, deformation diachronism and block rotations, Tectonophysics, 683, 308–324, doi:10.1016/j.tecto.2016.05.045, 2016.

Cunha, T. A., Matias, L. M., Terrinha, P., Negredo, A. M., Rosas, F., Fernandes, R. M. S. and Pinheiro, L. M.: Neotectonics of the SW Iberia margin, Gulf of Cadiz and Alboran Sea: a reassessment including recent structural, seismic and geodetic data: 530 Neotectonics SW Iberia-Gulf of Cadiz-Alboran, Geophysical Journal International, 188(3), 850–872, doi:10.1111/j.1365-246X.2011.05328.x, 2012.

Custódio, S., Lima, V., Vales, D., Cesca, S. and Carrilho, F.: Imaging active faulting in a region of distributed deformation from the joint clustering of focal mechanisms and hypocentres: Application to the Azores–western Mediterranean region, Tectonophysics, 676, 70–89, doi:10.1016/j.tecto.2016.03.013, 2016.

535 DeMets, C., Iaffaldano, G. and Merkouriev, S.: High-resolution Neogene and Quaternary estimates of Nubia-Eurasia-North America Plate motion, Geophys. J. Int., 203(1), 416–427, doi:10.1093/gji/ggv277, 2015.

Derder, M. E. M., Henry, B., Maouche, S., Bayou, B., Amenna, M., Besse, J., Bessedik, M., Belhai, D. and Ayache, M.: Transpressive tectonics along a major E–W crustal structure on the Algerian continental margin: Blocks rotations revealed by a paleomagnetic analysis, Tectonophysics, 593, 183–192, doi:10.1016/j.tecto.2013.03.007, 2013.

540 Díaz, J., Gil, A., Carbonell, R., Gallart, J. and Harnafi, M.: Constraining the crustal root geometry beneath Northern Morocco, Tectonophysics, 689, 14–24, doi:10.1016/j.tecto.2015.12.009, 2016.

Diaz, J., Gallart, J. and Carbonell, R.: Moho topography beneath the Iberian-Western Mediterranean region mapped from controlled-source and natural seismicity surveys, Tectonophysics, 692, 74–85, doi:10.1016/j.tecto.2016.08.023, 2016.

Dillon, W. P., Robb, J. M., Greene, H. G. and Lucena, J. C.: Evolution of the continental margin of southern Spain and the 545 Alboran Sea, Marine Geology, 36(3), 205–226, doi:10.1016/0025-3227(80)90087-0, 1980.

Do Couto, D.: Evolution géodynamique de la mer d'Alboran par l'étude des bassin sédimentaires, Université Pierre et Marie Curie, Paris, FRANCE, 16 January., 2014.

Do Couto, D., Gumiaux, C., Augier, R., Lebret, N., Folcher, N., Jouannic, G., Jolivet, L., Suc, J.-P. and Gorini, C.: Tectonic inversion of an asymmetric graben: Insights from a combined field and gravity survey in the Sorbas basin, Tectonics, 33(7), 550 2013TC003458, doi:10.1002/2013TC003458, 2014.

Do Couto, D., Gorini, C., Jolivet, L., Lebret, N., Augier, R., Gumiaux, C., d'Acremont, E., Ammar, A., Jabour, H. and Auxietre, J.-L.: Tectonic and stratigraphic evolution of the Western Alboran Sea Basin in the last 25 Myrs, Tectonophysics, 677–678, 280–311, doi:10.1016/j.tecto.2016.03.020, 2016.

Duggen, S., Hoernle, K., van den Bogaard, P. and Harris, C.: Magmatic evolution of the Alboran region: The role of subduction 555 in forming the western Mediterranean and causing the Messinian Salinity Crisis, Earth and Planetary Science Letters, 218(1–2), 91–108, doi:10.1016/S0012-821X(03)00632-0, 2004.

Duggen, S., Hoernle, K., Klügel, A., Geldmacher, J., Thirlwall, M., Hauff, F., Lowry, D. and Oates, N.: Geochemical zonation of the Miocene Alborán Basin volcanism (westernmost Mediterranean): geodynamic implications, Contributions to Mineralogy and Petrology, 156(5), 577–593, doi:10.1007/s00410-008-0302-4, 2008.

560 Dziewonski, A. M., Chou, T.-A. and Woodhouse, J. H.: Determination of earthquake source parameters from waveform data for studies of global and regional seismicity, J. Geophys. Res., 86(B4), 2825–2852, doi:10.1029/JB086iB04p02825, 1981.

Ekström, G., Nettles, M. and Dziewoński, A. M.: The global CMT project 2004–2010: Centroid-moment tensors for 13,017 earthquakes, Physics of the Earth and Planetary Interiors, 200–201, 1–9, doi:10.1016/j.pepi.2012.04.002, 2012.

El Alami, S. O., Tadili, B. A., Cherkaoui, T. E., Medina, F., Ramdani, M., Brahim, L. A. and Harnafi, M.: The Al Hoceima 565 earthquake of May 26, 1994 and its aftershocks: a seismotectonic study, ANALI DI GEOFISICA, 41(4), 519–537, 1998.

El Azzouzi, M., Bellon, H., Coutelle, A. and Réhault, J.-P.: Miocene magmatism and tectonics within the Peri-Alboran orogen (western Mediterranean), Journal of Geodynamics, 77, 171–185, doi:10.1016/j.jog.2014.02.006, 2014.

Ercilla, G., Juan, C., Hernández-Molina, F. J., Bruno, M., Estrada, F., Alonso, B., Casas, D., Farran, M., Llave, E., García, M., Vázquez, J. T., D'Acremont, E., Gorini, C., Palomino, D., Valencia, J., El Moumni, B. and Ammar, A.: Significance of bottom 570 currents in deep-sea morphodynamics: An example from the Alboran Sea, Marine Geology, doi:10.1016/j.margeo.2015.09.007, 2016.

Estrada, F., Ercilla, G., Gorini, C., Alonso, B., Vázquez, J. T., García-Castellanos, D., Juan, C., Maldonado, A., Ammar, A. and Elabbassi, M.: Impact of pulsed Atlantic water inflow into the Alboran Basin at the time of the Zanclean flooding, Geo-Marine Letters, 31(5–6), 361–376, doi:10.1007/s00367-011-0249-8, 2011.

575 Estrada, F., Vazquez, J. T., Ercilla, G., Alonso, B., d'Acremont, E., Gorini, C., Gomez, M., Fernandez-Puga, M. C., Ammar, A. and El Moumni, B.: Recent tectonic inversion of the Central Alboran Zone, Resúmenes de la 2ª Reunión Ibérica sobre Fallas Activas y Paleosismología, 51, 2014.

Estrada, F., Galindo-Zaldívar, J., Vázquez, Gemma, E., D'Acremont, E., Belén, B. and Gorini, C.: Tectonic indentation in the central Alboran Sea (westernmost Mediterranean), Terra Nova, 30(1), 24–33, doi:10.1111/ter.12304, 2018.

580 Fossen, H. and Tikoff, B.: Extended models of transpression and transtension, and application to tectonic settings, Geological Society, London, Special Publications, 135(1), 15–33, doi:https://doi.org/10.1144/GSL.SP.1998.135.01.02, 1998.

Fossen, H., Tikoff, B. and Teyssier, C.: Strain modeling of transpressional and transtensional deformation, Norsk Geologisk Tidsskrift, 74(3), 134–145, 1994.

Galindo-Zaldívar, J., González-Lodeiro, F. and Jabaloy, A.: Stress and palaeostress in the Betic-Rif cordilleras (Miocene to
585 the present), Tectonophysics, 227(1–4), 105–126, doi:10.1016/0040-1951(93)90090-7, 1993.

Galindo-Zaldívar, J., Azzouz, O., Chalouan, A., Pedrera, A., Ruano, P., Ruiz-Constán, A., Sanz de Galdeano, C., Marín-Lechado, C., López-Garrido, A., Anahnah, F. and Benmakhlouf, M.: Extensional tectonics, graben development and fault terminations in the eastern Rif (Bokoya–Ras Afraou area), Tectonophysics, 663, 140–149, doi:10.1016/j.tecto.2015.08.029, 2015.

590 Galindo-Zaldivar, J., Ercilla, G., Estrada, F., Catalán, M., d'Acremont, E., Azzouz, O., Casas, D., Chourak, M., Vazquez, J. T., Chalouan, A., Galdeano, C. S. de, Benmakhlouf, M., Gorini, C., Alonso, B., Palomino, D., Rengel, J. A. and Gil, A. J.: Imaging the Growth of Recent Faults: The Case of 2016–2017 Seismic Sequence Sea Bottom Deformation in the Alboran Sea (Western Mediterranean), Tectonics, 0(0), doi:10.1029/2017TC004941, 2018.

Garcia-Castellanos, D., Villasenor and A.: Messinian salinity crisis regulated by competing tectonics and erosion at the
595 Gibraltar arc, Nature, 480, 359–363, 2011.

Gensous, B., Tesson, M. and Winnock, E.: La marge meridionale de la mer d'alboran: caracteres structuro-sedimentaires et evolution recente, Marine Geology, 72, 341–370, doi:10.1016/0025-3227(86)90127-1, 1986.

Giaconia, F., Booth-Rea, G., Ranero, C. R., Gràcia, E., Bartolome, R., Calahorrano, A., Lo Iacono, C., Vendrell, M. G., Cameselle, A. L., Costa, S., Gómez de la Peña, L., Martínez-Loriente, S., Perea, H. and Viñas, M.: Compressional tectonic
600 inversion of the Algero-Balearic basin: Latemost Miocene to present oblique convergence at the Palomares margin (Western Mediterranean), Tectonics, 34(7), 2015TC003861, doi:10.1002/2015TC003861, 2015.

Gill, R. C. O., Aparicio, A., El Azzouzi, M., Hernandez, J., Thirlwall, M. F., Bourgois, J. and Marriner, G. F.: Depleted arc volcanism in the Alboran Sea and shoshonitic volcanism in Morocco: geochemical and isotopic constraints on Neogene tectonic processes, Lithos, 78(4), 363–388, doi:10.1016/j.lithos.2004.07.002, 2004.

605 Gràcia, E., Pallàs, R., Soto, J. I., Comas, M., Moreno, X., Masana, E., Santanach, P., Diez, S., García, M. and Dañobeitia, J.: Active faulting offshore SE Spain (Alboran Sea): Implications for earthquake hazard assessment in the Southern Iberian Margin, Earth and Planetary Science Letters, 241(3–4), 734–749, doi:10.1016/j.epsl.2005.11.009, 2006.

Gràcia, E., Bartolome, R., Lo Iacono, C., Moreno, X., Stich, D., Martínez-Diaz, J. J., Bozzano, G., Martínez-Loriente, S., Perea, H., Diez, S., Masana, E., Dañobeitia, J. J., Tello, O., Sanz, J. L., Carreño, E. and EVENT-SHELF Team: Acoustic and
610 seismic imaging of the Adra Fault (NE Alboran Sea): in search of the source of the 1910 Adra earthquake, Nat. Hazards Earth Syst. Sci., 12(11), 3255–3267, doi:10.5194/nhess-12-3255-2012, 2012.

Gràcia, E., Grevemeyer, I., Bartolomé, R., Perea, H., Martínez-Loriente, S., Peña, L. G. de la, Villaseñor, A., Klinger, Y., Iacono, C. L., Diez, S., Calahorrano, A., Camafort, M., Costa, S., d'Acremont, E., Rabaute, A. and Ranero, C. R.: Earthquake crisis unveils the growth of an incipient continental fault system, Nat Commun, 10(1), 1–12, doi:10.1038/s41467-019-11064-
615 5, 2019.

Grevemeyer, I., Gràcia, E., Villaseñor, A., Leuchters, W. and Watts, A. B.: Seismicity and active tectonics in the Alboran Sea, Western Mediterranean: Constraints from an offshore-onshore seismological network and swath bathymetry data, J. Geophys. Res. Solid Earth, 120(12), 2015JB012073, doi:10.1002/2015JB012073, 2015.

Hamai, L., Petit, C., Abtout, A., Yelles-Chaouche, A. and Déverchère, J.: Flexural behaviour of the north Algerian margin and
620 tectonic implications, Geophys. J. Int., 201(3), 1426–1436, doi:10.1093/gji/ggv098, 2015.

Hatzfeld, D., Caillot, V., Cherkaoui, T.-E., Jebli, H. and Medina: Microearthquake seismicity and fault plane solutions around
the Nékor strike-slip fault, Morocco, Earth and Planetary Science Letters, 120(1–2), 31–41, doi:https://doi.org/10.1016/0012-
821X(93)90021-Z, 1993.

Jolivet, L., Augier, R., Faccenna, C., Negro, F., Rimmele, G., Agard, P., Robin, C., Rossetti, F. and Crespo-Blanc, A.:
625 Subduction, convergence and the mode of backarc extension in the Mediterranean region, Bulletin de la Société Géologique
de France, 179(6), 525–550, doi:https://doi.org/10.2113/gssgfbull.179.6.525, 2008.

Jolivet, L., Faccenna, C. and Piromallo, C.: From mantle to crust: Stretching the Mediterranean, Earth and Planetary Science
Letters, 285(1–2), 198–209, doi:10.1016/j.epsl.2009.06.017, 2009.

Juan, C., Ercilla, G., Javier Hernández-Molina, F., Estrada, F., Alonso, B., Casas, D., García, M., Farran, M., Llave, E.,
630 Palomino, D., Vázquez, J.-T., Medialdea, T., Gorini, C., D'Acremont, E., El Moumni, B. and Ammar, A.: Seismic evidence
of current-controlled sedimentation in the Alboran Sea during the Pliocene and Quaternary: Palaeoceanographic implications,
Marine Geology, doi:10.1016/j.margeo.2016.01.006, 2016.

Judd, A. and Hovland, M.: Seabed Fluid Flow: The Impact on Geology, Biology and the Marine Environment, Cambridge
University Press., 2009.

635 Koulali, A., Ouazar, D., Tahayt, A., King, R. W., Vernant, P., Reilinger, R. E., McClusky, S., Mourabit, T., Davila, J. M. and
Amraoui, N.: New GPS constraints on active deformation along the Africa–Iberia plate boundary, Earth and Planetary Science
Letters, 308(1–2), 211–217, doi:10.1016/j.epsl.2011.05.048, 2011.

Koyi, H., Nilfouroushan, F. and Hessami, K.: Modelling role of basement block rotation and strike-slip faulting on structural
pattern in cover units of fold-and-thrust belts, Geological Magazine, 153(5–6), 827–844, doi:10.1017/S0016756816000595,
640 2016.

Lafosse, M., d'Acremont, E., Rabaute, A., Mercier de Lépinay, B., Tahayt, A., Ammar, A. and Gorini, C.: Evidence of
quaternary transtensional tectonics in the Nekor basin (NE Morocco), Basin Res, 29(4), 470–489, doi:10.1111/bre.12185,
2017.

Le Friant, A., Boudon, G., Komorowski, J.-C. and Deplus, C.: L'île de la Dominique, à l'origine des avalanches de débris les
645 plus   volumineuses   de   l'arc   des   Petites   Antilles,   Comptes   Rendus   Geoscience,   334(4),   235–243,
doi:https://doi.org/10.1016/S1631-0713(02)01742-X, 2002.

Le Friant, A., Boudon, G., Arnulf, A. and Robertson, R. E. A.: Debris avalanche deposits offshore St. Vincent (West Indies):
Impact of flank-collapse events on the morphological evolution of the island, Journal of Volcanology and Geothermal
Research, 179(1–2), 1–10, doi:10.1016/j.jvolgeores.2008.09.022, 2009.

650 Le Pourhiet, L., Huet, B. and Traoré, N.: Links between long-term and short-term rheology of the lithosphere: Insights from
strike-slip fault modelling, Tectonophysics, 631, 146–159, doi:10.1016/j.tecto.2014.06.034, 2014.

Leblanc, D. and Olivier, P.: Role of strike-slip faults in the Betic-Rifian orogeny, Tectonophysics, 101(3–4), 345–355,
doi:10.1016/0040-1951(84)90120-3, 1984.

Lisiecki, L. E. and Raymo, M. E.: A Pliocene-Pleistocene stack of 57 globally distributed benthic δ18O records,
655 Paleoceanography, 20(1), PA1003, doi:10.1029/2004PA001071, 2005.

Martínez-Díaz, J. J. and Hernández-Enrile, J. L.: Neotectonics and morphotectonics of the southern Almería region (Betic
Cordillera-Spain) kinematic implications, Int J Earth Sci (Geol Rundsch), 93(2), 189–206, doi:10.1007/s00531-003-0379-y,
2004.

Martínez-García, P., Soto, J. I. and Comas, M.: Recent structures in the Alboran Ridge and Yusuf fault zones based on swath
660 bathymetry and sub-bottom profiling: evidence of active tectonics, Geo-Marine Letters, 31(1), 19–36, doi:10.1007/s00367-
010-0212-0, 2011.

Martínez-García, P., Comas, M., Soto, J. I., Lonergan, L. and Watts, A. B.: Strike-slip tectonics and basin inversion in the
Western Mediterranean: the Post-Messinian evolution of the Alboran Sea, Basin Research, 25(4), 361–387,
doi:10.1111/bre.12005, 2013.

665   Martínez-García, P., Comas, M., Lonergan, L. and Watts, A. B.: From extension to shortening: tectonic inversion distributed in time and space in the Alboran Sea, Western Mediterranean: Tectonic inversion in the Alboran Sea, Tectonics, doi:10.1002/2017TC004489, 2017.

Medina, F. and Cherkaoui, T.-E.: The South-Western Alboran Earthquake Sequence of January-March 2016 and Its Associated Coulomb Stress Changes, Open Journal of Earthquake Research, 6(01), 35, 2017.

670   Meghraoui, M. and Pondrelli, S.: Active faulting and transpression tectonics along the plate boundary in North Africa, Ann. Geophys., 55(5), doi:10.4401/ag-4970, 2013.

Muñoz, A., Ballesteros, M., Montoya, I., Rivera, J., Acosta, J. and Uchupi, E.: Alborán Basin, southern Spain—Part I: Geomorphology, Marine and Petroleum Geology, 25(1), 59–73, doi:10.1016/j.marpetgeo.2007.05.003, 2008.

Neres, M., Carafa, M. M. C., Fernandes, R. M. S., Matias, L., Duarte, J. C., Barba, S. and Terrinha, P.: Lithospheric
675   deformation in the Africa-Iberia plate boundary: Improved neotectonic modeling testing a basal-driven Alboran plate, J. Geophys. Res. Solid Earth, 121(9), 2016JB013012, doi:10.1002/2016JB013012, 2016.

Nocquet, J.-M.: Present-day kinematics of the Mediterranean: A comprehensive overview of GPS results, Tectonophysics, 579, 220–242, doi:10.1016/j.tecto.2012.03.037, 2012.

Nocquet, J.-M. and Calais, E.: Geodetic Measurements of Crustal Deformation in the Western Mediterranean and Europe,
680   Pure and Applied Geophysics, 161(3), 661–681, doi:10.1007/s00024-003-2468-z, 2004.

Nur, A., Ron, H. and Scotti, O.: Fault mechanics and the kinematics of block rotations, Geology, 14(9), 746–749, doi:10.1130/0091-7613(1986)14<746:FMATKO>2.0.CO;2, 1986.

Palano, M., González, P. J. and Fernández, J.: Strain and stress fields along the Gibraltar Orogenic Arc: Constraints on active geodynamics, Gondwana Research, 23(3), 1071–1088, doi:10.1016/j.gr.2012.05.021, 2013.

685   Palano, M., González, P. J. and Fernández, J.: The Diffuse Plate boundary of Nubia and Iberia in the Western Mediterranean: Crustal deformation evidence for viscous coupling and fragmented lithosphere, Earth and Planetary Science Letters, 430, 439–447, doi:10.1016/j.epsl.2015.08.040, 2015.

Palomino, D., Vázquez, J.-T., Ercilla, G., Alonso, B., López-González, N. and Díaz-del-Río, V.: Interaction between seabed morphology and water masses around the seamounts on the Motril Marginal Plateau (Alboran Sea, Western Mediterranean),
690   Geo-Mar Lett, 31(5–6), 465–479, doi:10.1007/s00367-011-0246-y, 2011.

Paulatto, M., Watts, A. B. and Peirce, C.: Potential field and high-resolution bathymetry investigation of the Monowai volcanic centre, Kermadec Arc: implications for caldera formation and volcanic evolution, Geophys. J. Int., ggt512, doi:10.1093/gji/ggt512, 2014.

Peacock, D. C. P. and Sanderson, D. J.: Strike-slip relay ramps, Journal of structural geology, 17(10), 1351–1360,
695   doi:10.1016/0191-8141(95)97303-W, 1995.

Perea, H., Gràcia, E., Martínez-Loriente, S., Bartolome, R., de la Peña, L. G., de Mol, B., Moreno, X., Iacono, C. L., Diez, S., Tello, O., Gómez-Ballesteros, M. and Dañobeitia, J. J.: Kinematic analysis of secondary faults within a distributed shear-zone reveals fault linkage and increased seismic hazard, Marine Geology, 399, 23–33, doi:10.1016/j.margeo.2018.02.002, 2018.

Perouse, E., Vernant, P., Chery, J., Reilinger, R. and McClusky, S.: Active surface deformation and sub-lithospheric processes
700   in the western Mediterranean constrained by numerical models, Geology, 38(9), 823–826, doi:10.1130/G30963.1, 2010.

Petit, C., Pourhiet, L. L., Scalabrino, B., Corsini, M., Bonnin, M. and Romagny, A.: Crustal structure and gravity anomalies beneath the Rif, northern Morocco: implications for the current tectonics of the Alboran region, Geophys. J. Int., 202(1), 640–652, doi:10.1093/gji/ggv169, 2015.

Platt, J.P., Allerton, S., Kirker, A.I., Mandeville, C., Mayfield, A., Platzman, E., Rimi and A.: The ultimate arc: Differential
705   displacement, oroclinal bending, and vertical axis rotation in the External Betic-Rif arc, Tectonics, 22, 1017, 2003.

Poujol, A., Ritz, J.-F., Tahayt, A., Vernant, P., Condomines, M., Blard, P.-H., Billant, J., Vacher, L., Tibari, B., Hni, L. and Koulali, A.: Active tectonics of the Northern Rif (Morocco) from geomorphic and geochronological data, Journal of Geodynamics, 77, 70–88, doi:10.1016/j.jog.2014.01.004, 2014.

Reicherter, K. R. and Reiss, S.: The Carboneras Fault Zone (southeastern Spain) revisited with Ground Penetrating Radar-
710   Quaternary structural styles from high-resolution images, Geologie en Mijnbouw, 80(3/4), 129–138, 2001.

Roberts, A.: Curvature attributes and their application to 3 D interpreted horizons, First break, 19(2), 85–100, 2001.

Rodriguez, M., Maleuvre, C., Jollivet-Castelot, M., d'Acremont, E., Rabaute, A., Lafosse, M., Ercilla, G., Vázquez, J.-T., Alonso, B. and Ammar, A.: Tsunamigenic submarine landslides along the Xauen–Tofiño banks in the Alboran Sea (Western Mediterranean Sea), Geophysical Journal International, 209(1), 266–281, doi:https://doi.org/10.1093/gji/ggx028, 2017.

715 Roldán, F. J., Galindo-Zaldívar, J., Ruano, P., Chalouan, A., Pedrera, A., Ahmamou, M., Ruiz-Constán, A., Sanz de Galdeano, C., Benmakhlouf, M., López-Garrido, A. C., Anahnah, F. and González-Castillo, L.: Basin evolution associated to curved thrusts: The Prerif Ridges in the Volubilis area (Rif Cordillera, Morocco), Journal of Geodynamics, 77, 56–69, doi:10.1016/j.jog.2013.11.001, 2014.

Romagny, A., Ph. Münch, Cornée, J.-J., Corsini, M., Azdimousa, A., Melinte-Dobrinescu, M. C., Drinia, H., Bonno, M.,
720 Arnaud, N., Monié, P., Quillévéré, F. and Ben Moussa, A.: Late Miocene to present-day exhumation and uplift of the Internal Zone of the Rif chain: Insights from low temperature thermochronometry and basin analysis, Journal of Geodynamics, 77, 39–55, doi:10.1016/j.jog.2014.01.006, 2014.

Ron, H., Beroza, G. and Nur, A.: Simple model explains complex faulting, Eos Trans. AGU, 82(10), 125–129, doi:10.1029/EO082i010p00125-01, 2001.

725 Ruiz-Constán, A., Galindo-Zaldívar, J., Pedrera, A., Célérier, B., Marín-Lechado and C.: Stress distribution at the transition from subduction to continental collision (northwestern and central Betic Cordillera), Geochem. Geophys. Geosyst., 12, Q12002, doi:10.1029/2011gc003824, 2011.

Scholz, C. H., Ando, R. and Shaw, B. E.: The mechanics of first order splay faulting: The strike-slip case, Journal of Structural Geology, 32(1), 118–126, doi:10.1016/j.jsg.2009.10.007, 2010.

730 Soto, I., J., Fernandez-Ibanez, Fermin, Talukder, Asrar, Martinez-Garcia, Pedro and Anonymous: Miocene shale tectonics in the Alboran Sea (western Mediterranean), Abstracts with Programs - Geological Society of America, 40, 187, 2008.

Soto, J. I., Fernández-Ibáñez, F. and Talukder, A. R.: Recent shale tectonics and basin evolution of the NW Alboran Sea, The Leading Edge, 31(7), 768–775, doi:https://doi.org/10.1190/tle31070768.1, 2012.

Spakman, W., Chertova, M. V., van den Berg, Arie. and van Hinsbergen, D. J. J.: Puzzling features of western Mediterranean
735 tectonics explained by slab dragging, Nature Geoscience, doi:10.1038/s41561-018-0066-z, 2018.

Sternai, P., Caricchi, L., Garcia-Castellanos, D., Jolivet, L., Sheldrake, T. E. and Castelltort, S.: Magmatic pulse driven by sea-level changes associated with the Messinian salinity crisis, Nature Geoscience, 10(10), 783–787, doi:10.1038/ngeo3032, 2017.

Stich, D., Mancilla, F. d. L., Baumont, D. and Morales, J.: Source analysis of the Mw 6.3 2004 Al Hoceima earthquake (Morocco) using regional apparent source time functions, Journal of Geophysical Research, 110(B6),
740 doi:10.1029/2004JB003366, 2005.

Stich, D., Serpelloni, E., de Lis Mancilla, F. d. L. and Morales, J.: Kinematics of the Iberia–Maghreb plate contact from seismic moment tensors and GPS observations, Tectonophysics, 426(3–4), 295–317, doi:10.1016/j.tecto.2006.08.004, 2006.

Stich, D., Martín, R. and Morales, J.: Moment tensor inversion for Iberia–Maghreb earthquakes 2005–2008, Tectonophysics, 483(3–4), 390–398, doi:10.1016/j.tecto.2009.11.006, 2010.

745 Storti, F., Soto Marin, R., Rossetti, F. and Casas Sainz, A. M.: Evolution of experimental thrust wedges accreted from along-strike tapered, silicone-floored multilayers, Journal of the Geological Society, 164(1), 73–85, doi:10.1144/0016-76492005-186, 2007.

Tadayon, M., Rossetti, F., Zattin, M., Calzolari, G., Nozaem, R., Salvini, F., Faccenna, C. and Khodabakhshi, P.: The long-term evolution of the Doruneh Fault region (Central Iran): A key to understanding the spatio-temporal tectonic evolution in
750 the hinterland of the Zagros convergence zone, edited by C. Frassi, Geological Journal, doi:10.1002/gj.3241, 2018.

Tesson, M., Gensous, B. and Lambraimi, M.: Seismic analysis of the southern margin of the Alboran Sea, Journal of African Earth Sciences (1983), 6(6), 813–821, doi:10.1016/0899-5362(87)90038-8, 1987.

Thurner, S., Palomeras, I., Levander, A., Carbonell, R. and Lee, C.-T.: Ongoing lithospheric removal in the western Mediterranean: Evidence from Ps receiver functions and thermobarometry of Neogene basalts (PICASSO project),
755 Geochemistry, Geophysics, Geosystems, 15(4), 1113–1127, doi:10.1002/2013GC005124, 2014.

Van der Woerd, J., Dorbath, C., Ousadou, F., Dorbath, L., Delouis, B., Jacques, E., Tapponnier, P., Hahou, Y., Menzhi, M., Frogneux, M. and Haessler, H.: The Al Hoceima Mw 6.4 earthquake of 24 February 2004 and its aftershocks sequence, Journal of Geodynamics, 77, 89–109, doi:10.1016/j.jog.2013.12.004, 2014.

Vázquez, J. T., Estrada, F., Vegas, R., Ercilla, G., d'Acremont, E., Fernández-Salas, L. M. and Alonso, B.: Quaternary tectonics influence onthe Adra continental slope morphology (northern Alboran Sea), 2014.

Vernant, P., Fadil, A., Mourabit, T., Ouazar, D., Koulali, A., Davila, J. M., Garate, J., McClusky, S. and Reilinger, R.: Geodetic constraints on active tectonics of the Western Mediterranean: Implications for the kinematics and dynamics of the Nubia-Eurasia plate boundary zone, Journal of Geodynamics, 49(3–4), 123–129, doi:10.1016/j.jog.2009.10.007, 2010.

Watts, A. B., Platt, J. P. and Buhl, P.: Tectonic evolution of the Alboran Sea basin, Basin Research, 5(3), 153–177, doi:https://doi.org/10.1111/j.1365-2117.1993.tb00063.x, 1993.

11. Figures
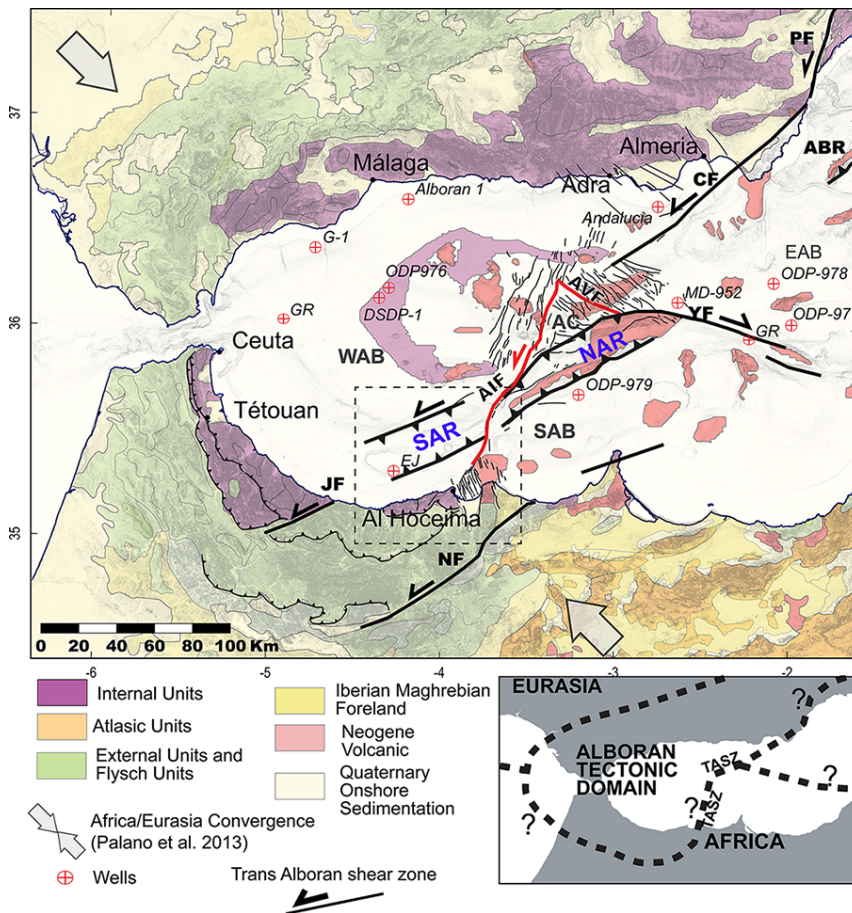
Figure 1. Topographic map and principal structural units of the Alboran region. Structural units in the studied area modified from Chalouan et al., (2008); Comas et al., (1999); Leblanc and Olivier, (1984); Romagny et al., (2014). The Trans Alboran Shear Zone (TASZ) indicates the motion inferred for the Late-Miocene – Pliocene period. The red faults are the present-day active Al-Idrissi fault and its conjugated Averroes Fault. AC, Alboran Channel; AVR, Averroes Fault; ABR, Abubacer Ridge; CF, Carboneras Fault, EAB; East Alboran Basin; AIF, Al-Idrissi Fault; JF, Jebha fault; NF, Nekor Fault; SAB, South Alboran Basin; SAR, South Alboran Ridge; NAR, North Alboran Ridge; YF, Yusuf Fault; WAB, West Alboran Basin. Inset: Hypotheses of plate boundaries between an Alboran tectonic domain and the African plate from Nocquet, (2012).
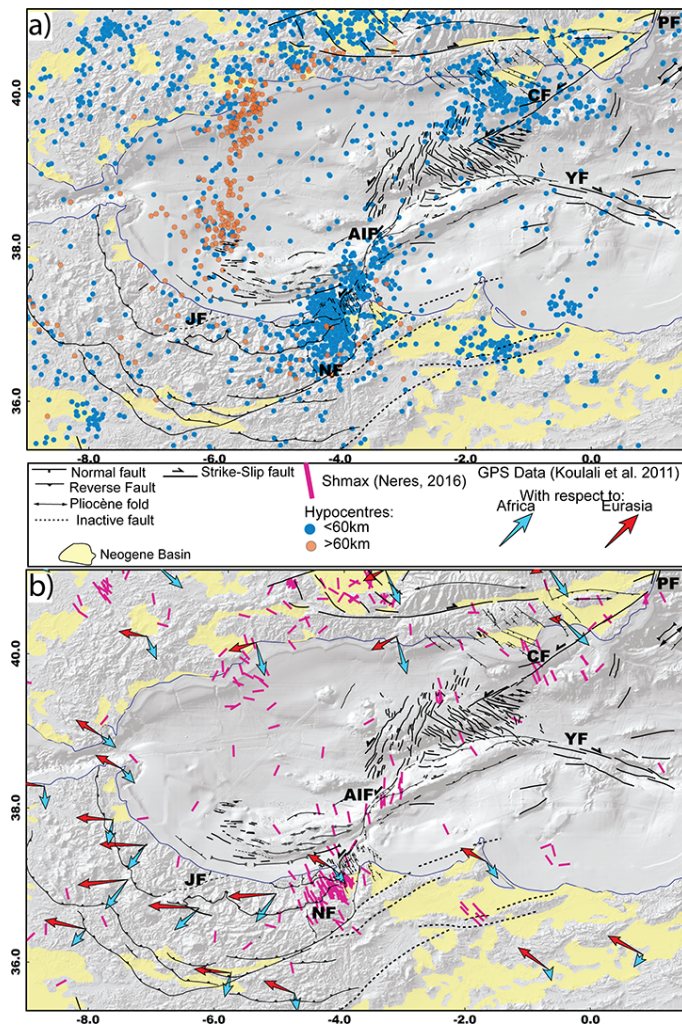
Figure 2. Maps showing the distribution of the seismicity along the Neogene tectonic structures in the Alboran Sea. a) Neotectonic map of the Alboran region modified from d'Acremont et al., (2014), Alvarez-Marrón and others, (1999), Chalouan et al., (1997), Estrada et al., (2014), Gràcia et al., (2006), (2012); Lafosse et al., (2016), Martínez-García et al., (2011), Muñoz et al., (2008), Perea et al., (2014); Vázquez et al., (2014) and from this study. Seismicity from IGN catalogue 1970-2017 (http://www.ign.es/), only earthquakes with Mw >= 3 and depth >=2 km are figured. b) GPS data from Koulali et al., (2011) and Sh_{max} from Neres et al., (2016). See figure 1 for scale. CF, Carboneras fault; PF, Palomares fault; YF, Yusuf fault; NF, Nekor fault; AIF, Al-Idrissi fault zone.
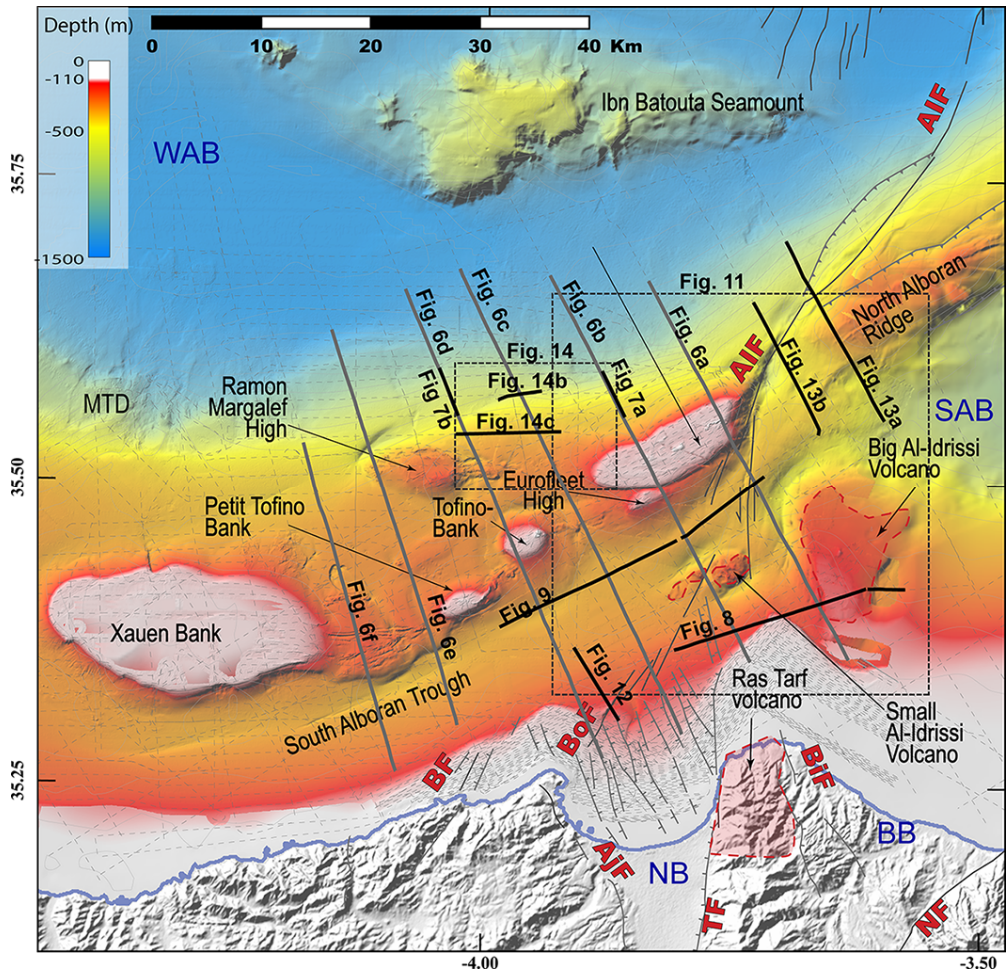
785

Figure 3. Bathymetry of the studied area showing the main morpho-structural features of the studied area. Dark grey and black lines, positions of the seismic lines used in the study. MTD, Mass Transport Deposits; WAB, West Alboran Basin; SAB, South Alboran Basin; BB, Boudinar Basin; BF: Boussekkour Fault; Bof, Bokoya Fault; BiF, Boudinar Fault; NB, Nekor Basin; NF, Nekor Fault; AIF; Al-Idrissi Fault zone; TF, Trougout fault; AjF, Adjir-Imzouren Fault.

790
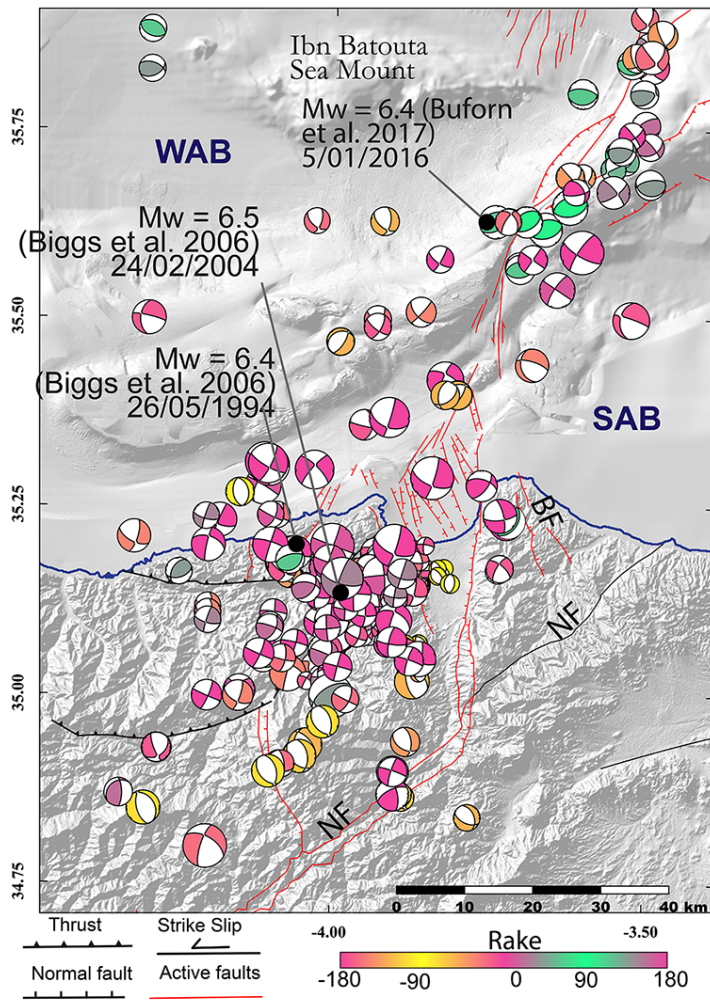
Figure 4. Map of the distribution of the present-day deformation showing strike-slip and compressive deformation along the northern part of the studied area and extensional and strike-slip structures along the southern part. Focal mechanism till 2014 period from the compilation of Custódio et al.(2016) and for the year 2016 from GCMT project (http://www.globalcmt.org/; Dziewonski et al., 1981; Ekström et al., 2012). The size of the focal mechanisms corresponds to the magnitude values (from Mw= 2.3 to 6.4). Structural data compiled from Ballesteros et al., (2008); Biggs et al., (2006); Buforn et al., (2017); Chalouan et al., (1997); Lafosse et al., (2017) and Martínez-García et al., (2011). BF, Boudinar Fault, WAB, West Alboran Basin; SAB, South Alboran Basin; NF, Nekor fault.
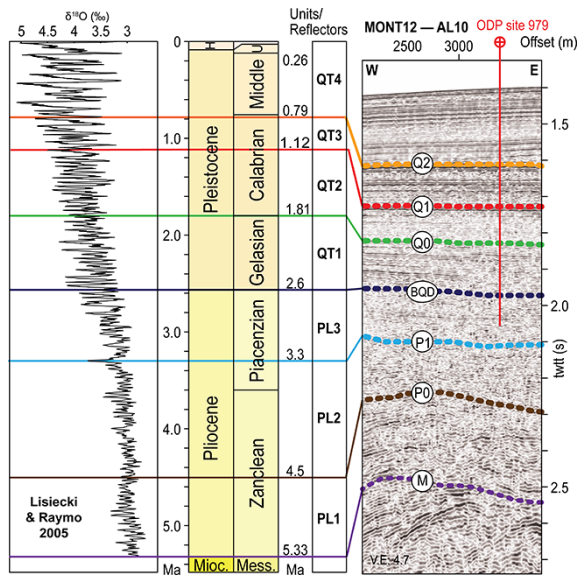
Figure 5. Well log correlation to the seismic section, seismic line crossing the location of the ODP 979 site, vertical stacking of the Pliocene and Quaternary units, and available δ¹⁸O curve from Lisiecki and Raymo (2005). The colors of the stratigraphic surfaces are the same as in the following seismic lines.

805
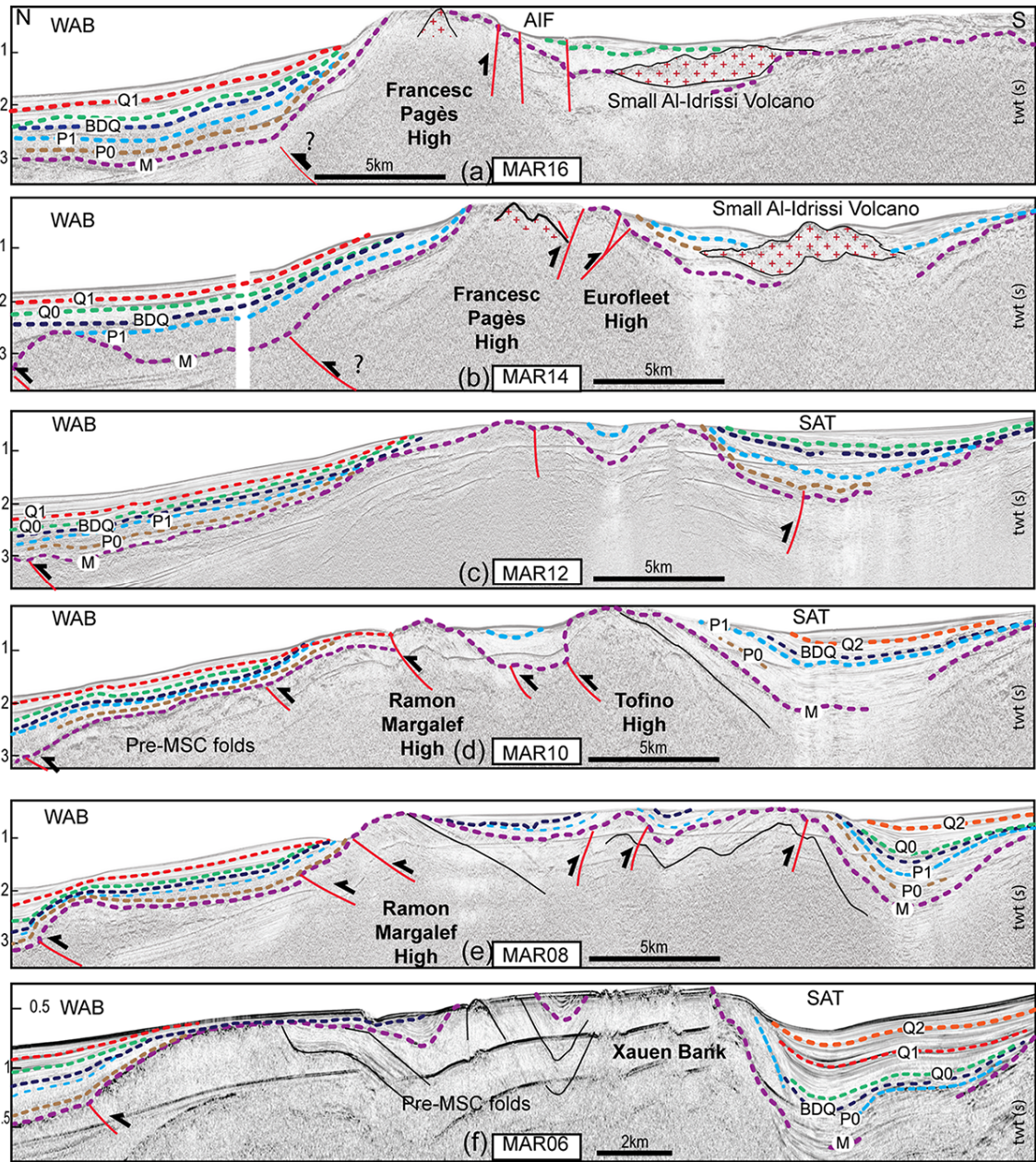
Figure 6. Multichannel seismic lines showing the Plio-Quaternary stratigraphy and structural features. Dashed and colored lines are the stratigraphic surface defined in figure 5. Black reflectors, pre-MSC reflectors. The seismic section (a) to (f) are ordered from east to west. WAB, South Alboran Basin; SAT, South Alboran Trough; AIF, Al-Idrissi Fault zone.

810
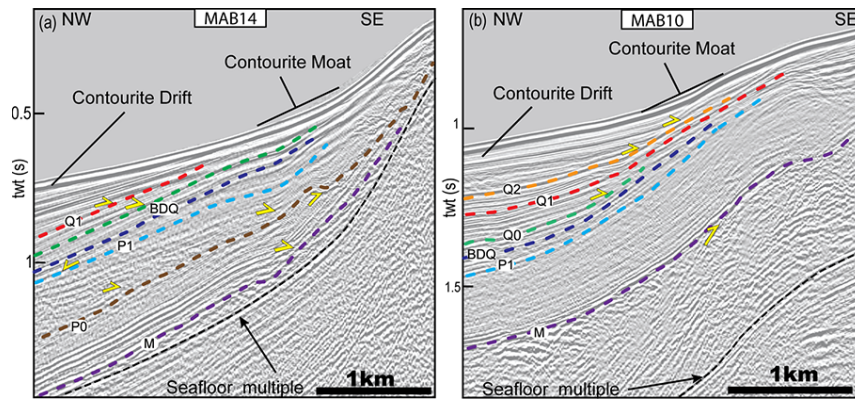
Figure 7: Seismic unconformities at the foot slope of the northern flank of the South Alboran Ridge. a) Seismic line at the foot of the Francesc Pagès bank. b) Seismic line at the foot of the Ramon Margalef high. The seismic lines show the diachronism of the deformation affecting the SAR during the Pliocene. After 2.6 Ma, the moats of the contourites pinch at the feet of the folds.

815
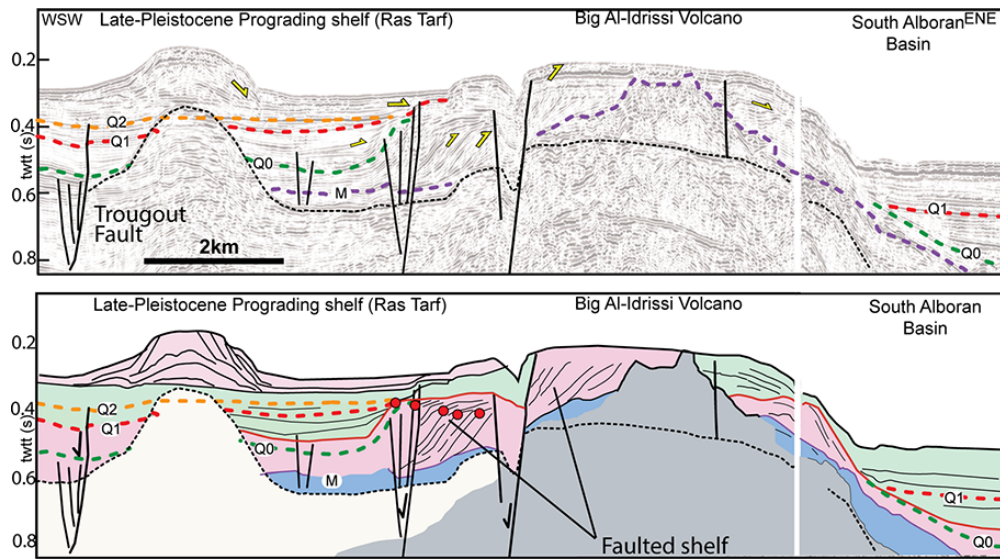
Figure 8: Multichannel seismic profile showing the transgression of marine sediment (in green) over the prograding shelf to the edges of the Big Al-Idrissi volcano (in pink) crossing the Ras Tarf Promontory and the Big Al-Idrissi Volcano. Dashed black reflector, multiple of the seafloor. Red points, offlap break (Paleo-shore line) marking the concave up trajectories of the offlap breaks and progradation of the shelf and the first transgression before 1.81Ma. The red surface is a maximum regressive surface in the sense of Catuneanu et al. (2011). The seismic line shows the transgression of marine sediment (in green) over the Pliocene to Quaternary prograding shelf to the edges of the Big Al-Idrissi volcano (in pink). Older depositional units are colored in blue and the acoustic basement in grey.

820
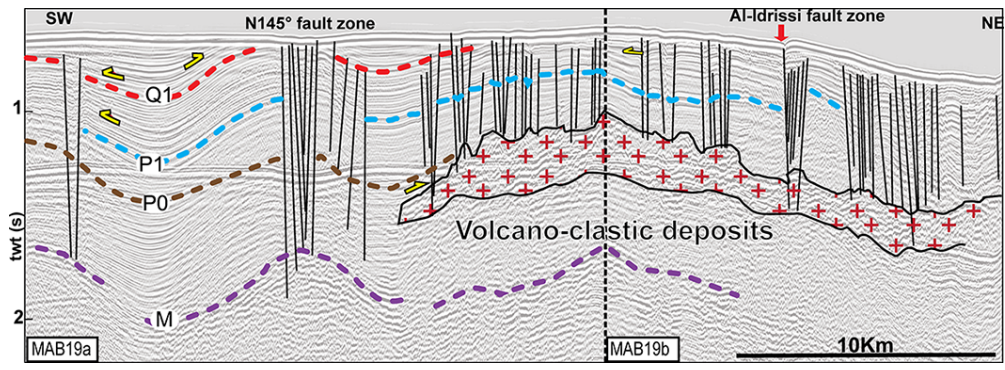
825

Figure 9. Multichannel seismic profile showing seismic stratigraphy and the main structural elements along a portion of the South Alboran Trough located between N145° striking faults and the AIF. Line track on figure 3. (a) Raw seismic line (b) Interpreted seismic line. Red-crosses in b) figure a seismic body made of poorly continuous high-amplitude reflectors interpreted as volcano-
830 **clastic deposits.**
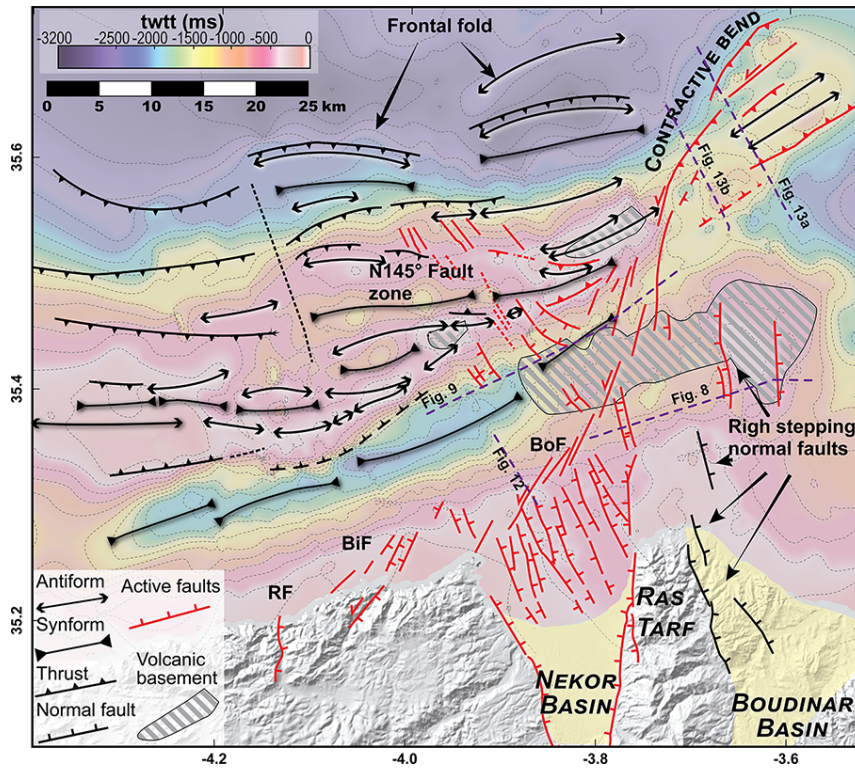
Figure 10: Structural map of Plio-Quaternary faults and folds overlying the map of depths of the Messinian unconformity. Active faults correspond to the faults affecting the seafloor. BF: Boussekkour Fault; Bof, Bokoya Fault; RF, Rouadi Fault.

835
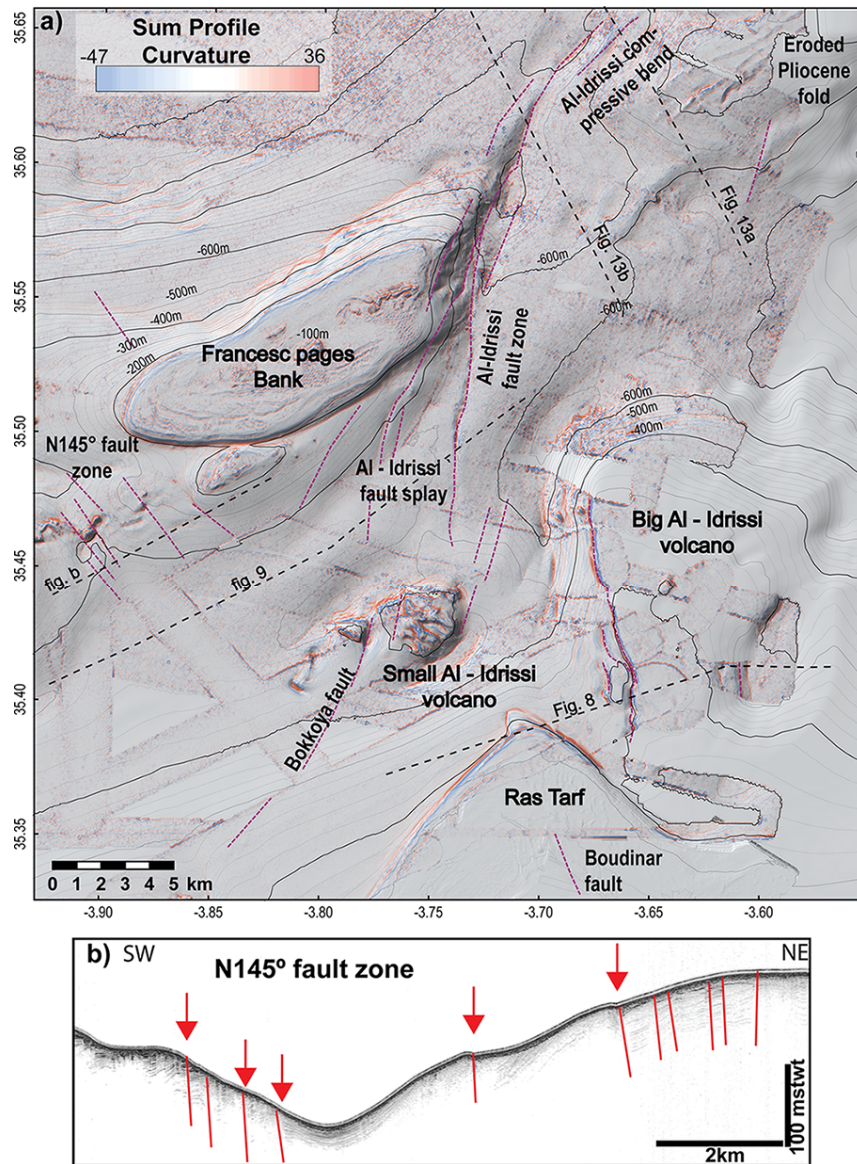
Figure 11: Active structures around the roughly NNE-SSW AIF and adjacent submarine highs. The AIF bends to the North, where it follows the trends of the NAR. High values of curvatures in the Francesc Pagès Bank and the Northeast corner of the map underline the linear features at the seafloor, which corresponds to the truncated Miocene-Pliocene layers. Extreme positive values in red represent concave topography at the seafloor; extreme negative values in blue represent convex topography. a) Profile curvature map textured above the shaded bathymetry; dashed purple lines, fault tracks at the seafloor; dashed black lines, positions of the seismic line in (b) and in figures 8, 9, and 13. b) TOPAS profile showing active N145° normal faults. Red lines, active faults; red arrows, positions of the fault traces in (a).
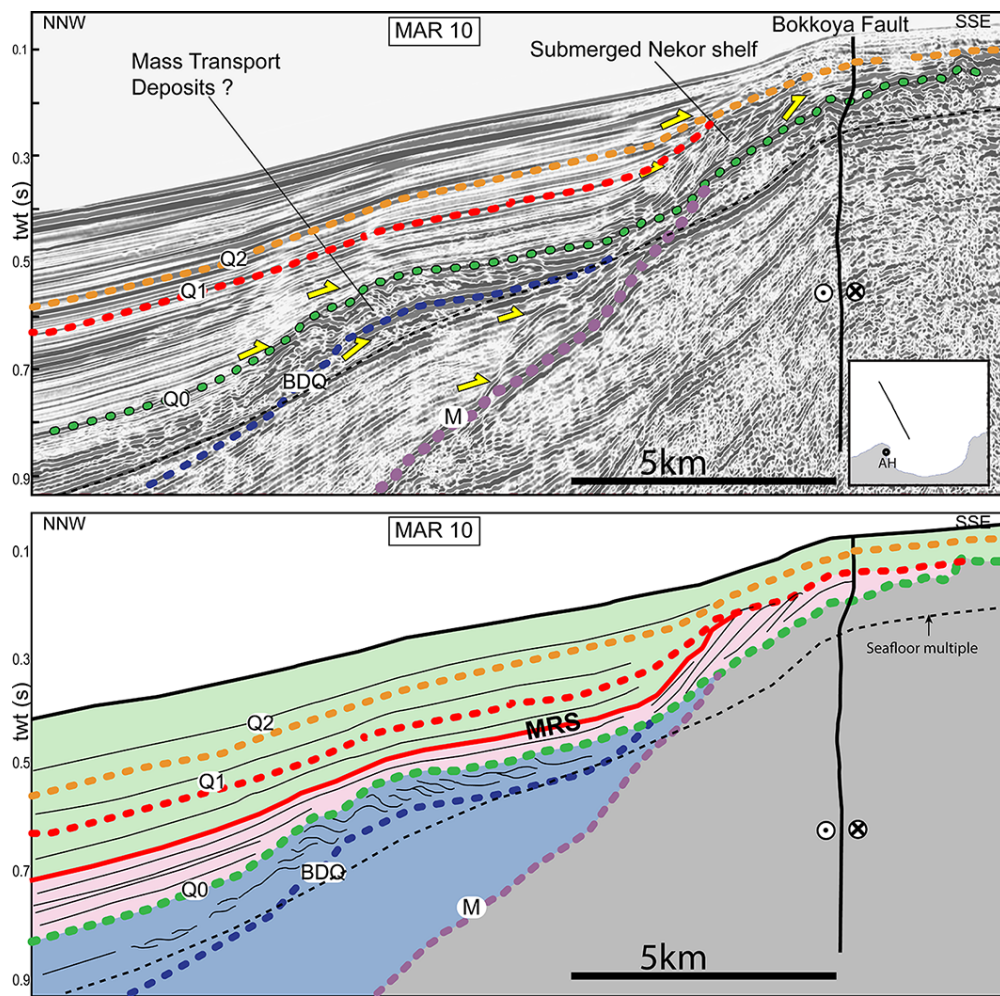
Figure 12: SPARKER seismic line showing the transgression of marine sediment (in green) over the prograding shelf of the Nekor Basin (in pink). Oldest depositional units (Pliocene) are colored in blue and the acoustic basement in grey. The Maximum Regressive Surface (MRS) is in red.

850
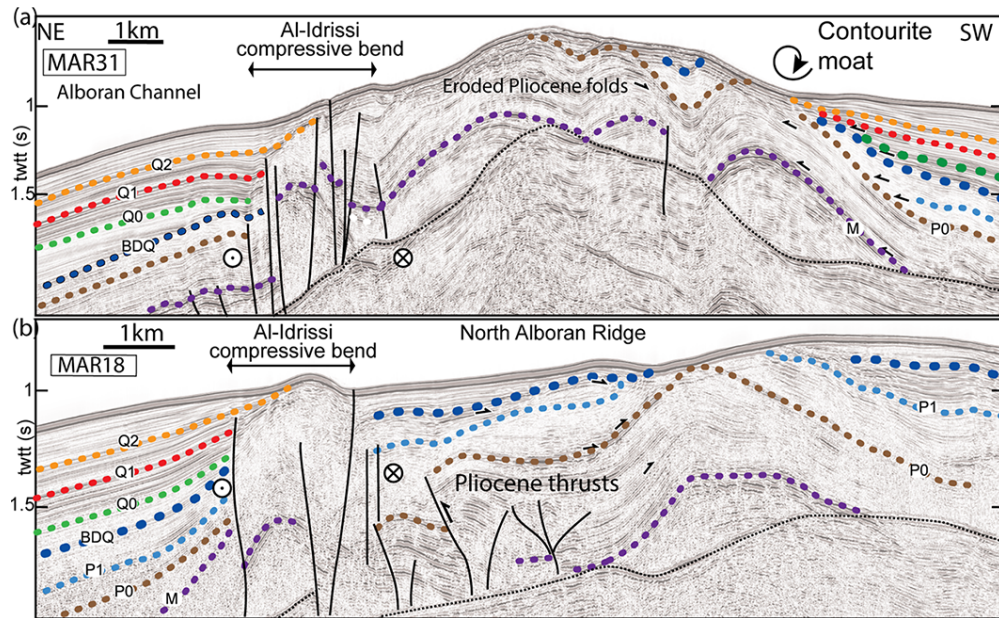
Figure 13: Multichannel seismic lines across the compressional bend of the Al-Idrissi fault zone showing lateral evolution of the tectonic structures in North Alboran Ridge and in the compressional bend. a) The Al-Idrissi fault zone is a positive flower structure following the front of the Alboran Ridge. b) The Al-Idrissi fault zone is a positive flower structure distinct from the Pliocene thrusts and folds.

855
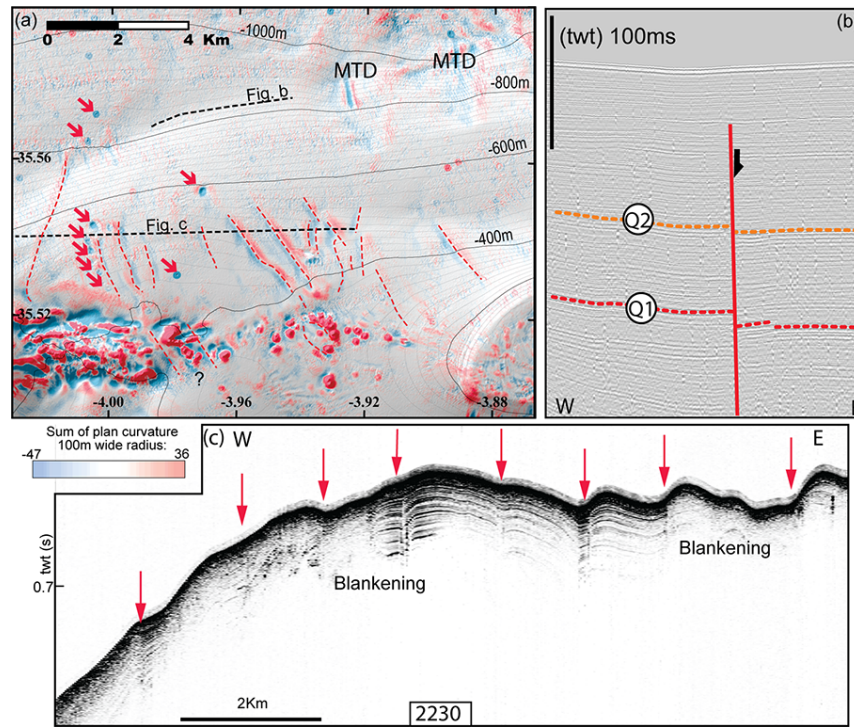
Figure 14: Active structures affecting the northern flank of Francesc Pagès and Ramon Margalef highs. a) plan curvature map overlying the shaded bathymetry; red arrows pockmarks on the seafloor; dashed black lines, seismic lines in the figures (b) and (c); dashed red lines, positions of the fault tracks. b) SPARKER seismic reflection line showing the northward continuity of N145° fault (red line). c) TOPAS seismic line showing the subsurface of the seafloor. Red arrows, positions of the faults drawn in a).
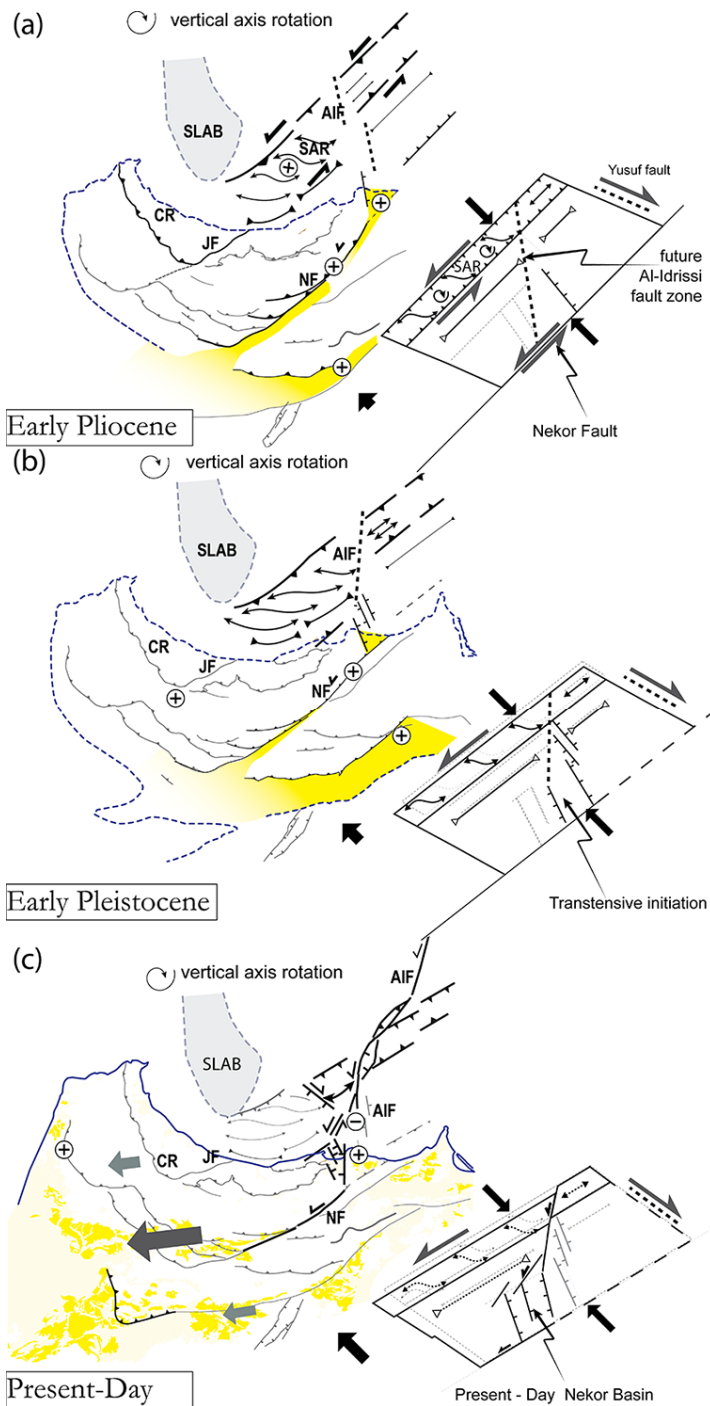
865 **Figure 15: Palinspastic maps of the SAR and the Rif from 5 Ma to the present-day are using 14 ° clockwise rotation of the Alboran tectonic domain from a) to c). Dashed blue line, approximate coastline; continuous blue line, present-day coastline; Dark yellow, Miocene-Pliocene onshore basins; light yellow, Pliocene and Quaternary onshore basins; grey patch, position of the slab remaining approximatively constant below the Alboran Basin during the Plio-Quaternary; left bottom corner of the maps, simplified drawing figure the area between the SAR, the Nekor fault and the Yusuf fault. Thick grey arrows in (c) indicate the direction and relative 870 amount of extrusion in the central Rif considering a fixed Eurasia. The shortening is accommodated through compressive structures in (a). The initiation of subsidence along the Big Al-Idrissi Volcano and the Moroccan shelf corresponds to (b), and the present–day partitioning of the deformation corresponds to (c). CR, central Rif, JF, Jebha Fault; NF, Nekor Fault; AIF, Al-Idrissi Fault zone.**